STM JOURNALS

Journal of
Materials & Metallurgical Engineering

https://journals.stmjournals.com/jomme

ISSN: 2231-3818 (Online)
ISSN: 2321-4236 (Print)
Volume 14, Issue 3, 2024
September–December
DOI (Journal): 10.37591/JoMME

Review JoMME

Gelatin-E_iO_2 (E_i = Si/Ti/Zr) Based Mesoporous Nano-Hybrids: Synthesis and Characterization

Samjeet Singh Thakur[1,*]

Abstract

Hybrid materials are mostly prepared by combining the organic or bio-organic part to the inorganic building blocks and are used in many applications. Gelatin as one of the main components of hybrid materials is an attractive option. It is biodegradable, biocompatible, non-toxic, bio-adhesive, and contains many active groups such as –NH_2, –COOH, which in the biopolymer backbone makes these hybrid materials important in various technological applications. The synthesis of a series of gelatin-based nano-hybrid mesoporous materials was carried out using gelatin as the bio-polymeric backbone, silica, titania, or zirconia; sodium dodecyl sulfate (SDS) as surfactant for oil/water emulsion, tetraethly orthosilicate (TEOS) as silylation or cross-linker material to obtain different hybrid materials for different applications. Hydrochloric acid (HCl) was used as catalyst, n-hexane as the solvent and SDS as a surfactant for oil-water emulsification. Herein, sol-gel technique was used to prepare the mesoporous gelatin-E_iO_2 (E_i = Si/Ti/Zr) based mesoporous nano-hybrids which are promising and efficient. Thus, four kinds of different gelatin-based hybrid materials: gelatin-silica, modified gelatin-silica, gelatin-titania, and gelatin–zirconia based hybrid materials were synthesized. The effect of post-calcination on the properties of the as-synthesized hybrid materials was also studied and confirmed from various characterization techniques such as: elemental analysis, scanning electron microscopy (SEM), transmission electron microscopy (TEM), X-ray diffraction (XRD), thermogravimetric analysis (TGA), energy dispersive X-ray (EDX), and Fourier transform infrared (FTIR) spectroscopy and Brunauer-Emmett-Teller (BET) surface area analysis. To sum up, the materials synthesized are nano-hybrids which are mesoporous as confirmed from the various characterization techniques like SEM-EDS, have high surface area and are good candidates for many frontline applications.

Keywords: Nano-hybrid, hybrid material, gelatin, silica, titania, zirconia, mesoporous, characterization

INTRODUCTION

Chemists are able to create new functional hybrid materials with improved qualities and modify a wide variety of molecular species. In fact, a variety of techniques have been employed to exploit soft chemical pathways to synthesis and process the hybrid materials based on gelatin.

***Author for Correspondence**
Samjeet Singh Thakur
E-mail: samar23chem@gmail.com

[1]Assistant Professor, Department of Chemistry, Netaji Subhash Chandra Bose Memorial Utkrisht Govt. College Hamirpur, Himachal Pradesh, India

Received Date: September 03, 2024
Accepted Date: September 27, 2024
Published Date: October 12, 2024

Citation: Samjeet Singh Thakur. Gelatin-E_iO_2 (E_i = Si/Ti/Zr) Based Mesoporous Nano-Hybrids: Synthesis and Characterization. Journal of Materials & Metallurgical Engineering. 2024; 14(3): 31–64p.

These procedures involve the polymerization of metallic alkoxides, macro-monomers, and functional organo-silanes; the encapsulation of organic components within organo-silicas or hybrid metallic oxides derived from sol-gel; the organic fictionalization of lamellar-structured compounds such as nano-fillers or nano-clays; self-assembly or template growth; nano-building block approaches; hydrothermally processed hybrid zeolites or micro-porous metal-organic frameworks; integrative synthesis or coupled processes; bio-inspired strategies, etc. Depending on the concentration of the biopolymer, the pH of the solution, and the

concentration of the silica precursor, the aforementioned process can be used to generate materials of the core/shell gelatin/silica or silica/gelatin type.

The sol-gel process is a popular choice for the synthesis of gelatin-based hybrid materials due to its ease of use and controllability. Smitha et al. have reported the synthesis of biocompatible hydrophobic silica–gelatin based nano-hybrid materials by using sol–gel process [1]. General accepted strategies for the synthesis of hybrid materials using sol–gel procedure have been widely discussed in several articles [2–13]. Thin-film coating, powder synthesis, and the alteration of electrode surfaces or electrode/ electrolyte interfaces have all been accomplished using sol-gel procedures. This process typically produces micro-pore particle and surface area between 30 m^2/g and 900 m^2/g. The above-mentioned method produces hybrid materials with remarkable qualities like a large surface area, high porosity, high mechanical strength, and low modulus of elasticity. As a result, the composition, processing, optical, mechanical, and biodegradation stability of hybrid materials are incredibly versatile [14–18].

Reetz et al. reported a sol–gel procedure to encapsulate lipases in hydrophobic hybrid organic–inorganic matrices obtained through hydrolysis and co-condensation of $R–Si(OR)_3$ and tetraethyl orthosilicate (TEOS) [19]. Various composite materials and hybrid materials have been developed in recent years as support for the enzyme immobilizations [20–24] and drug delivery applications [25–29]. The large inner surface area of such hybrid materials, their excellent pore accessibility, and their ability to get functionalized with different complexing agents and chelating ligands make these materials ideal for use as adsorbents for the removal of toxic metal ions [30–34] and reactive dyes [35–38] from the waste water treatment. Moriones et al. [39] reported gas separation of organic binary mixtures by phenyl stationary phases using silica based organic–inorganic hybrid materials.

Among other biodegradable biopolymers, gelatin has been found to be a good chemical entity in the synthesis of hybrid materials. Gelatin-based hybrid materials are an interesting class of biomaterials. Their structures resemble biological macromolecular components. Since, gelatin is non-immunogenic and biodegradable and therefore, it was selected as the biopolymer backbone.

Gelatin has been suitably modified to various forms of hybrid materials for use in varied applications. It has good cross-linking ability due to the presence of zwitter-ionic structure of peptides and therefore, it has ability to hold a large amount of water that facilitates protein adsorption as well as provide mesoporous polymeric network allowing the controllable permeability for different applications. The biodegradability, biocompatibility and other unique properties of gelatin have been used in a variety of fields such as pharmaceutics, as adsorbent and as support for the enzyme immobilization. Due to the applications of hybrid materials synthesized from gelatin in various fields and it has adaptability in a wide range of applications, hence it was chosen as the main component for the synthesis of a new series of hybrid materials reported in this article.

The hybrid materials exhibit favorable physical characteristics, biocompatibility, pH and temperature sensitivity, and flexibility in synthesis. These attributes make them valuable for a range of applications, including waste water treatment, drug delivery supports, bio-separation and purification technologies, and immobilization of diverse biological species.

In the present study, synthesis of different hybrid materials with gelatin, gelatin-silica, gelatin-titania and gelatin-zirconia, as the main components using TEOS was accomplished by the sol-gel method. In this article the terms hybrid materials and hybrid matrices are used interchangeably in the text as these convey the same meaning.

This work describes the chemistry and techniques involved in creating bio-hybrid nanomaterials based on gelatin and inorganic oxides, such as silica (SiO_2), titania (TiO_2), and zirconia (ZrO_2). TEOS is used as the silylation material, and the solvent system is *n*-hexane and de-ionized water. The colorless

liquid known as TEOS is mostly utilized as a cross-linking agent in silicone polymers and hybrid materials, where it undergoes hydrolysis to yield SiO_2 using the sol-gel technique. SiO_2, TiO_2, and ZrO_2, among other inorganic oxides, are crystalline solids that are white in color and melt at approximately 1650°C, 1843°C, and 2715°C, in that order. Their hybrid materials function as an effective flocculent and provide excellent adsorbents for metal ions and dyes. SiO_2, TiO_2, and ZrO_2 are inorganic oxides that are surface active components; in addition, they provide hydrophobicity to the hybrid materials, which increases their mechanical strength. Several physical and chemical techniques were used to characterize each of the produced hybrid materials.

The main steps used are detailed below:

1. Creation of hybrid materials based on gelatin, using *n*-hexane as the solvent system and de-ionized water as the backbone.
2. Inorganic oxides, such as zirconia (ZrO_2), titania (TiO_2), and silica (SiO_2), were employed to improve the hybrid materials' porosity and surface characteristics.
3. Cross-linking reactions were carried out using TEOS as cross-linker.
4. Hydrochloric acid (HCl) was used as catalyst.
5. Sodium dodecyl sulfate (SDS) is a surface acting agent which is used in order to get mesoporous reduced size nanoparticles and to avoid agglomeration.
6. Various techniques, including thermogravimetric analysis (TGA), energy-dispersive X-ray spectroscopy (EDS or EDX) for elemental analysis or chemical characterization of a sample, scanning electron microscopy (SEM), transmission electron microscopy (TEM), X-ray diffraction (XRD), and Fourier transform infrared spectroscopy (FTIR) were used to characterize the synthesized hybrid materials.
7. The most significant characteristic of these materials is their micro-level interaction with water as a result of changes in temperature and pH in the surrounding environment.

EXPERIMENTAL

Materials

Gelatin bacteriological (Glaxo India Ltd., Mumbai, India), TEOS (Sigma-Aldrich, Germany), hydrochloric acid (RANKEM), SDSsuprapure, and *n*-hexane (SD Fine Chemicals Ltd., Mumbai, India), silicon dioxide, titanium dioxide, zirconium dioxide (Himedia Laboratories Pvt. Ltd., Mumbai, India) – all the chemicals used were of analytical grade. In all experiments, doubly de-ionized distilled water was used throughout. Chemical reactor with stirring and heating (Mini Block^{TM}, Germany) was used for stirring purpose at fixed temperature during the synthesis process as shown in Figure 1. Figure 2 displays the chemical structures of the surfactant (SDS), cross-linker (TEOS), and organic biopolymer backbone (gelatin) employed in this investigation.

Synthesis of Gelatin-Based Hybrid Materials

In the first series, gelatin-based mesoporous bio-hybrid nano-material was prepared with the emulsion method in two stages following a reported protocol [40–43]. Ten grams (10 g) of TEOS was dissolve in 20 mL of *n*-hexane in the first step. Then the catalyst was added, and 0.1 mL of 5% HCl (by weight) was added. For 30 minutes at room temperature, the ingredients of the chemical reactor were mixed. Using SDS, 0.15 g) as the surfactant and 5 g of gelatin, 140 mL of *n*-hexane, 50 mL doubly de-ionized water, and 16 g HCl (by weight) created the oil/water emulsion in the second stage. In the chemical reactor, the components were once more agitated for 30 minutes at room temperature according to the previous description. In this case, the emulsion was formed using a surfactant and hydrogen chloride (HCl) functions as a catalyst for the hydrolyzation. Moreover, an increase in HCl concentration lowers the interfacial tension without affecting the solution's viscosity. To begin the hydrolytic polycondensation of the oligopoly (TEOS) droplets, the contents from both stages were combined. This produced solid spheres of silica and gelatin, which were then integrated onto the beads. After being aged for 120 hours at 37°C, the combination precipitated out of the solution. Following a thorough washing in acetone, methanol, and water, the separated particles were maintained in a vacuum oven at 100°C for half an hour. For eight hours, a portion of each synthesized sample was calcined at 550°C. The resulting hybrid materials were designated as H_1 (as-synthesized) and H_{11} (calcined).

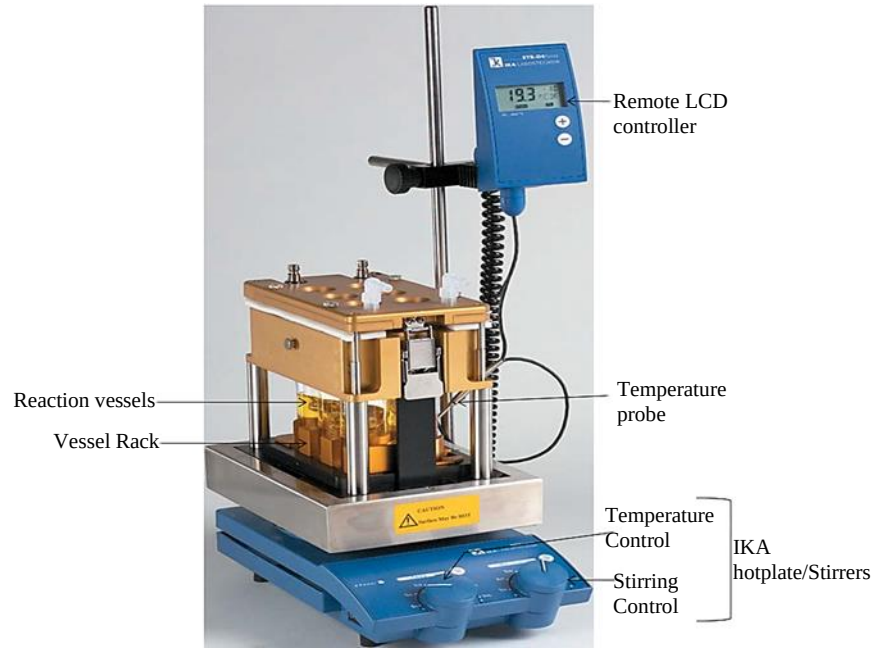

Figure 1. Chemical reactor with stirring and heating.

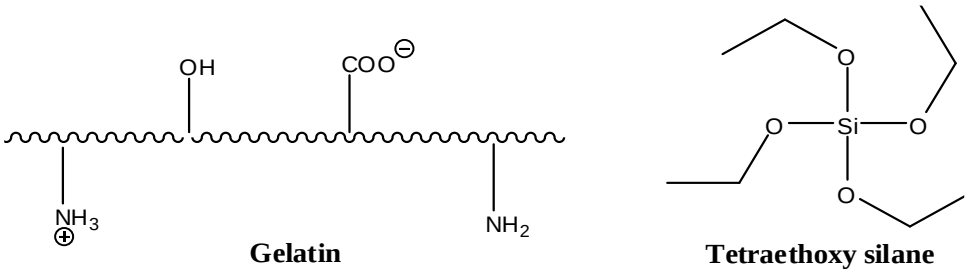

Gelatin **Tetraethoxy silane**

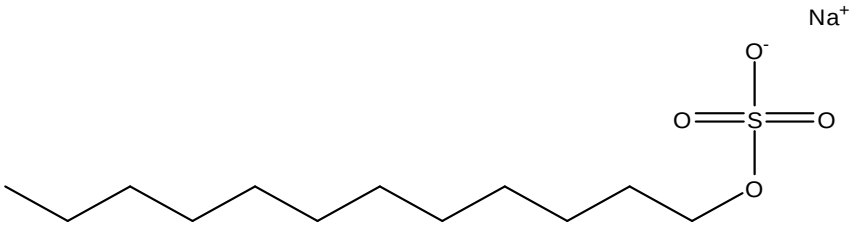

Sodium dodecyl sulphate

Figure 2. Structure of gelatin, tetraethyl orthosilicate (TEOS), and sodium dodecyl sulfate (SDS).

In the second series, a mesoporous bio-hybrid nanomaterial based on gelatin and silica was created using the emulsion process in two phases. First, 2.5 g of gelatin and SiO_2 were added to the gelatin in a 1:1 weight ratio to replace the original gelatin composition. Initially, 20 mL of *n*-hexane were used to dissolve 10 g of TEOS. Next, 2.5 g of SiO_2 was added after 0.1 mL of 5% HCl (by weight) was added as the catalyst. For 30 minutes at room temperature, the ingredients of the chemical reactor were mixed. It leads to the hydrolysis of TEOS to form silica network and rest of the reaction conditions used were same. The resulting hybrid materials were designated as H_2 (as-synthesized) and H_{22} (calcined).

In the third series, gelatin-titania based mesoporous bio-hybrid nanomaterial were prepared with the emulsion method in two stages where the composition of the gelatin was replaced to 1:1 weight ratio with 2.5 g each of gelatin and TiO_2. Rest of the procedure was followed as in the case of preceding series. The resulting hybrid materials were designated as H_3 (as-synthesized) and H_{33} (calcined).

Comparably, the emulsion method was used to prepare the fourth series of gelatin-zirconia based mesoporous bio-hybrid nanomaterial in two stages. The process for the second series was followed to replace the gelatin composition in a 1:1 weight ratio with 2.5 g of each of gelatin and ZrO_2. The resulting hybrid materials were designated as H_4 (as-synthesized) and H_{44} (calcined).

Characterization of Gelatin-Based Hybrid Material

Materials synthesized were characterized by using elemental analysis, FTIR spectroscopy, thermogravimetric/differential thermal analysis (TGA/DTA), XRD analysis, SEM-EDS, TEM, and Brunauer–Emmett–Teller (BET) analysis. Elemental analysis was recorded using Elemental Analyzer Vario EL CHNS. FTIR spectra were recorded on Nicolete 5700 in transmittance mode in KBr. TGA/DTA was carried out in TGA/DTA 6300, SII EXSTAR thermal analyzer. The thermal investigation was carried by heating samples from 50°C to 700°C in a platinum crucible in air atmosphere, heating at a rate of 10°C/min. XRD patterns of these hybrids were recorded on Bruker D-8 ADVANCE Diffractometer ($Cu–K_\alpha$ radiation with $\lambda = 1.54$ Å, 40 kV, 30 Am). The diffraction angle (2θ) was varied from 5° to 70°. Surface morphology of the samples was observed by scanning electron microscopy (Model: Leica Cambridge Stereoscan 440 SEM) and EDS were recorded on SEM QUANTA 250 D9393. The percentage weight of carbon, nitrogen, oxygen and silicon were also analyzed from the EDAX data. Transmission electron microscopy (TEM) images were taken using Philips model CM 200 which was operated with a copper electron source at an accelerating voltage of up to 200 kV (resolution: 2.4 Å, magnification range 5 to 300×). Surface area and pore size of the hybrid materials was analyzed using BET surface area analyzer with SMART SORB 92/93. The sample was degassed at 100°C before making the measurement.

RESULTS AND DISCUSSION

The relationship between structure and property in the networks of hybrid materials is contingent upon the reaction conditions utilized during synthesis, in addition to the impact of gelatin and cross-linkers such as TEOS. The chain length of the hybrid material is determined by the concentration of gelatin, TEOS, HCl (used as a catalyst), the solvent system, and the amount of surfactant (SDS) applied. The cross-linker's concentration controls the cross-linking density and porosity of the network created. The hybrid material's yield and network efficiency are also dependent on a number of reaction parameters, including temperature and pH. Gelatin was used as the swelling agent in a number of hybrid materials that were created due of its superior hydrophilicity and biological compatibility. It is an excellent option for creating mesoporous bio-hybrid nanomaterials because of its inexpensive cost.

Mechanism of Hybrid Materials Formation

The basic unit of gelatin represents the active groups like $=NH_2^+$ and $–COO^–$ and SiO_2, TiO_2, and ZrO_2 surfaces are shown in Figure 3. The functional moieties in the candidate materials make them capable of undergoing ionic, van der Waal interactions, and hydrogen bonding, etc., between the inorganic and organic constituents, resulting in hybrid materials.

The first step of the synthesis of the hybrid material is hydrolysis and condensation of TEOS [44]. The hydrolysis and condensation of TEOS leads to the formation of silica network as shown in Figure 4. This step is common to all series. The next step is different for all the four series as represented below in different schemes from Figure 5 to Figure 6. The synthesis of first series involves the formation of silica–gelatin hybrid material with TEOS as cross-linker using sol-gel method as shown in Figure 5. The synthesis of other series involves modified silica–gelatin, titania–gelatin, zirconia–gelatin hybrid materials as shown in Figure 6.

Siloxane based hybrids can be easily synthesized because Si–O–C (sp^3) bonds are covalent which are not broken upon easily upon hydrolysis. Similar chemistry is not applicable to transition metals for which the ionic M–O–C (Ti–O–C or Zr–O–C) bond is easily cleaved upon hydrolysis. Therefore,

hydrolysis of TEOS leads to the formation of silica network which get deposited onto the surface of titania or zirconia and therefore the silica primer coating and bonding to the biopolymer avoids the direct formation of ionic M–O–C (Ti–O–C or Zr–O–C) bond rather Ti–O–Si–O–C (sp^3) or Zr–O–Si–O–C (sp^3) covalent bond formation. Biopolymer backbone is used as the complexing organic ligand.

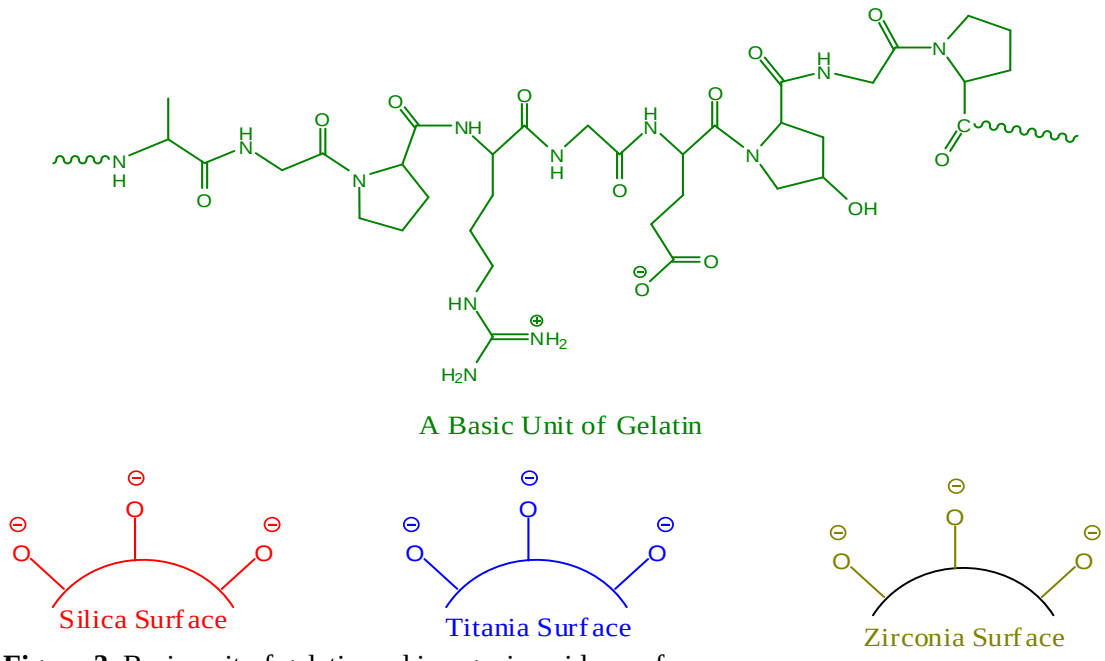

Figure 3. Basic unit of gelatin and inorganic oxides surface.

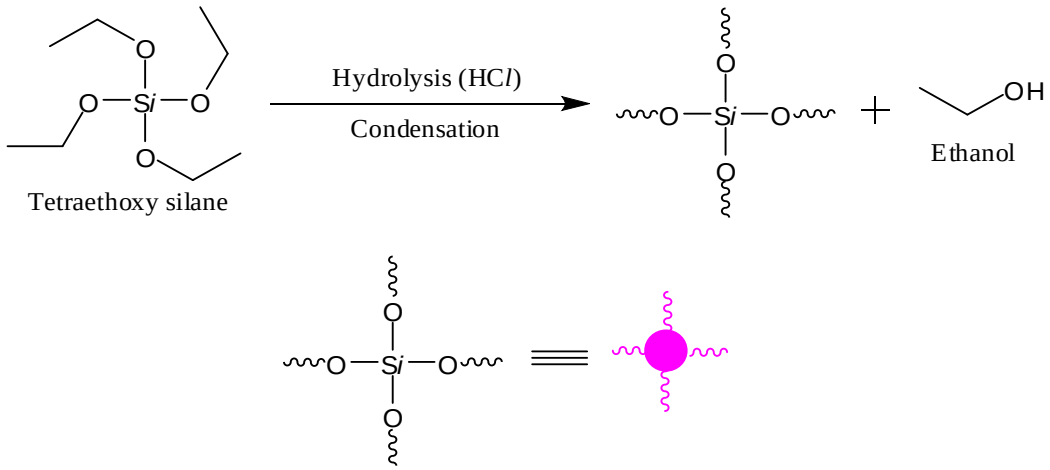

Figure 4. Silica-network formation by hydrolysis and condensation reaction of TEOS.

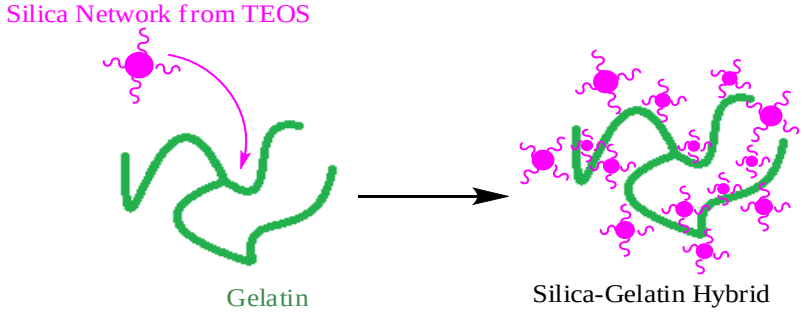

Figure 5. Formation of Silica-gelatin hybrid.

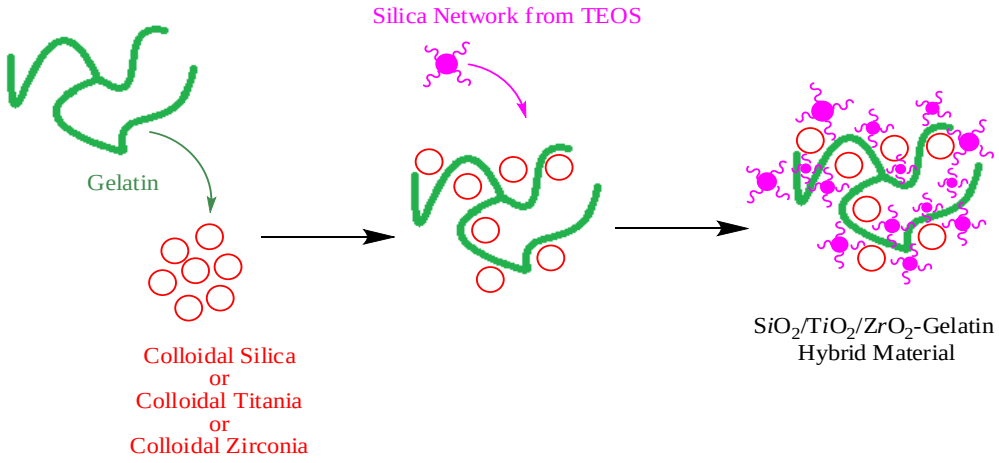

Figure 6. Formation of gelatin-EiO_2 based mesoporous nano-hybrid material.

Table 1. Elemental analysis.

S. No.	Hybrid Materials (Sample Codes)	Weight (mg)	C/N Ratio	CHNS Analysis			
				Carbon %	Nitrogen %	Hydrogen %	Sulfur %
1	H_1	4.8470	0.603	0.575	0.954	2.549	0.000
2	H_{11}	3.900	0.134	0.222	1.658	3.388	0.000
3	H_2	4.1700	0.878	2.479	2.825	1.497	0.000
4	H_{22}	4.3130	0.085	0.236	2.785	1.480	0.000
5	H_3	5.1370	0.496	1.747	3.525	1.794	0.000
6	H_{33}	4.9630	0.046	0.159	3.493	1.404	0.000
7	H_4	4.1480	0.361	2.130	5.905	2.571	0.000
8	H_{44}	5.1090	0.042	0.219	5.200	1.680	0.000

These groups can be functionalized for any type of organic reaction, including hybrid organic–inorganic copolymers formed through organic polymerization. The suggested mechanism of the network formation is as discussed and is provided in Figure 7. This is because the potential mechanism for the synthesis of the gelatin-silica, modified gelatin-silica, modified gelatin-titania, and modified gelatin-zirconia based hybrid material has been explained diagrammatically.

Characterization of Synthesized Hybrid Materials

Synthesized three-dimensional hybrid materials were characterized by the physical and chemical methods. The high cross-linking density, as well as the high percentage yield (almost equal to the total mass of the backbone, monomers, and cross-linker taken), confirms high conversion and the utility of the 'green synthetic protocol' used in this study. The photographs of hybrid materials taken at high magnification provide the clinching evidence of their formation. The use of CHNS analysis, FTIR, XRD, TGA, SEM–EDAX, TEM, and BET analysis techniques also confirms the network formation.

Elemental Analysis

Results of the CHN-analysis of different series of the hybrid materials are presented in Table 1. The presence of CHN confirms that all the series of hybrid materials contain gelatin, because gelatin is the backbone consist up of various amino acids. Sulfur is an additional element found in certain amino acids, such as cysteine and methionine. Since the amino acid cysteine is absent in the gelatin whereas methionine is found to be less than one percent (0.7%). Therefore, sulfur traces are not found during the CHNS analysis. Thus, satisfactory elemental analysis of the materials listed for all the hybrid material series confirms the formation of the gelatin-based hybrid materials.

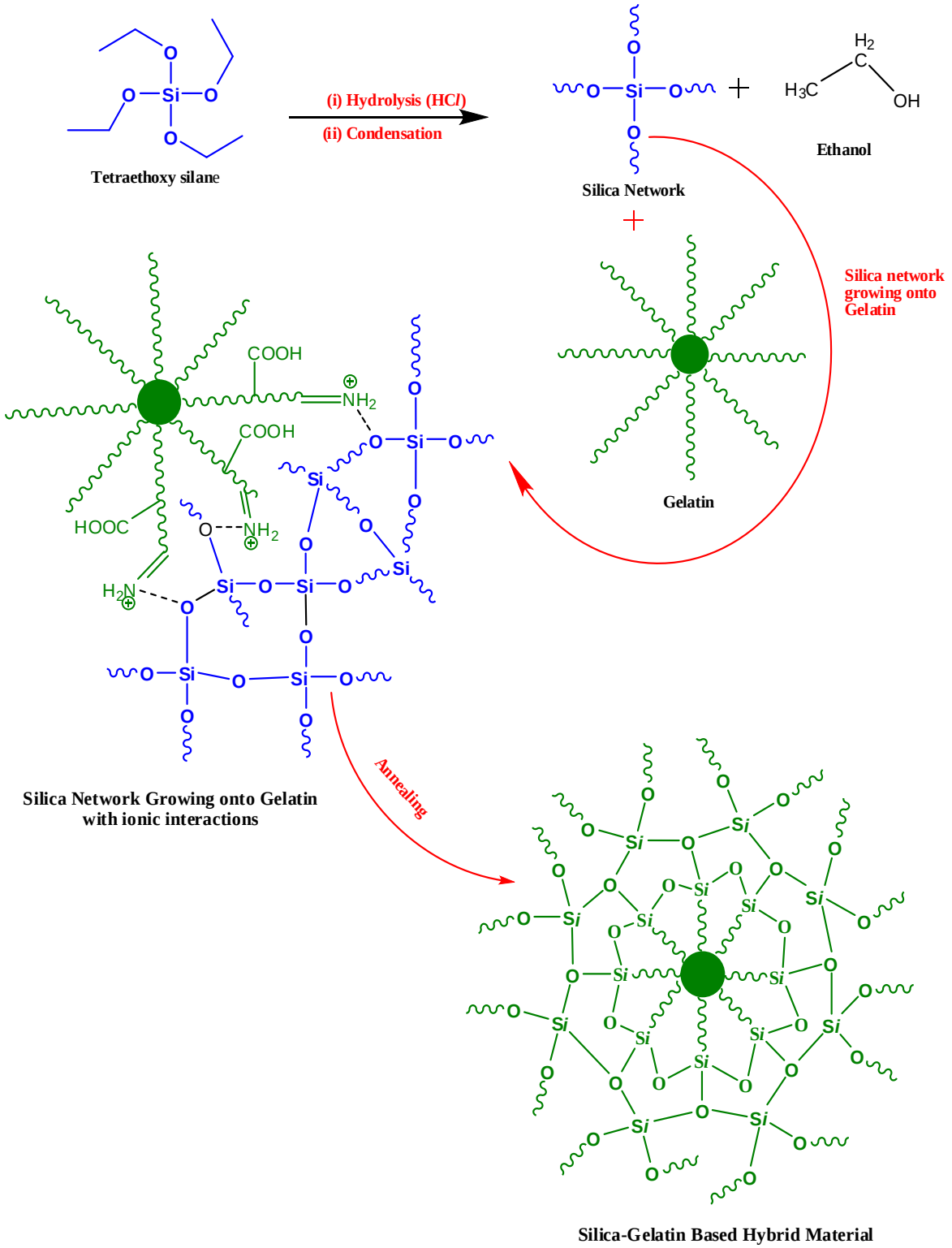

Figure 7. Proposed mechanism of the network formation.

Fourier Transform Infrared Studies

FTIR spectroscopy was used to characterize the hybrid materials, which are displayed in Figures 8 to 12. The FTIR spectra of the synthesized hybrid materials provide evidence of the network formation, as the additional characteristic peaks of the functional groups of different components appear in the resultant networks. The pure gelatin absorbs at 3428.7 cm^{-1}, 2925.5 cm^{-1}, 1103 cm^{-1} due to –OH or

secondary $–NH_2$, –CH and C–O stretching, respectively, as shown in Figure 8. Gelatin also shows two amide bands at 1684 cm^{-1} (C=O stretching of secondary amide) and 1555 cm^{-1} (–NH bending) [45]. The FTIR spectra of the gelatin–silica hybrid (H_1 and H_{11}) has broad band around 3450 cm^{-1} that corresponds to $–NH_2$ (2°) stretching as shown in Figure 9. The peaks between 1300 cm^{-1} to 1050 cm^{-1} are due to C–O stretching and two amide bands present in gelatin are reduced to only one peak in the hybrid at 1640 cm^{-1} (C=O stretching of secondary amide), Below 800 cm^{-1} the peaks are due to –NH deformation (out of plane) near 780 cm^{-1}, and Si–O stretching (700–400 cm^{-1}). Almost similar trends were observed for the FTIR spectra of the modified gelatin–silica hybrid materials (H_2 and H_{22}) as shown in Figure 10. But for the third and fourth hybrid series slight shifts to right or left were observed as shown in Figures 11 and 12. In the modified gelatin–titania hybrid materials (H_3 and H_{33}) one additional absorption bands at 1097 cm^{-1} corresponds to Si–O–Ti.

Sabataityte et al. [41] reported that below 500 cm^{-1}, the bands were assigned to Ti–O–Ti. In the modified gelatin–zirconia hybrid (H_4 and H_{44}) the sharp peaks near 800 cm^{-1} correspond to Zr–O–Si whereas the stretching band of Zr–O–Zr appears around 460 cm^{-1}. A band situated around 440 cm^{-1} is assigned to Zr–O–Zr in tetragonal zirconia. It is very weak below 500°C, as the vibration of Zr–O–Si exists between the bands of ZrO_2 and SiO_2 stretching [46]. The –NH bending mode has been missing in all the hybrids which may be due to ionic, van der Waals interactions between $=NH_2^+$ of the biopolymer backbone and O^- of the silica, titania, or zirconia surfaces. All the hybrids also show C=N stretching peak around 2300 cm^{-1}. The FTIR spectra of calcined materials (H_{11}, H_{22}, H_{33}, H_{44}) have less noise than those of as-synthesized (H_1, H_2, H_3, H_4) which is due to the unstable molecules and impurities. The stretching vibration of the Si–O–Si bridges shows the most intensive band, at 1100 cm^{-1} [47]. The peak splits into two separate bands at 1030 and 1130 cm^{-1} in the hybrid structures which may be due to the fictionalization of silanols through siloxane bridges by methyl groups.

In summary, it can be articulated that the existence of extra absorption peaks of the functional groups of the biopolymeric and inorganic components inserted in the network established provides a positive inference in favor of modifying gelatin and forming a network or hybrid materials. Additionally, a change in the location and intensity of distinctive backbone peaks in various networks indicates a variation of the biopolymer backbone or network creation [48, 49].

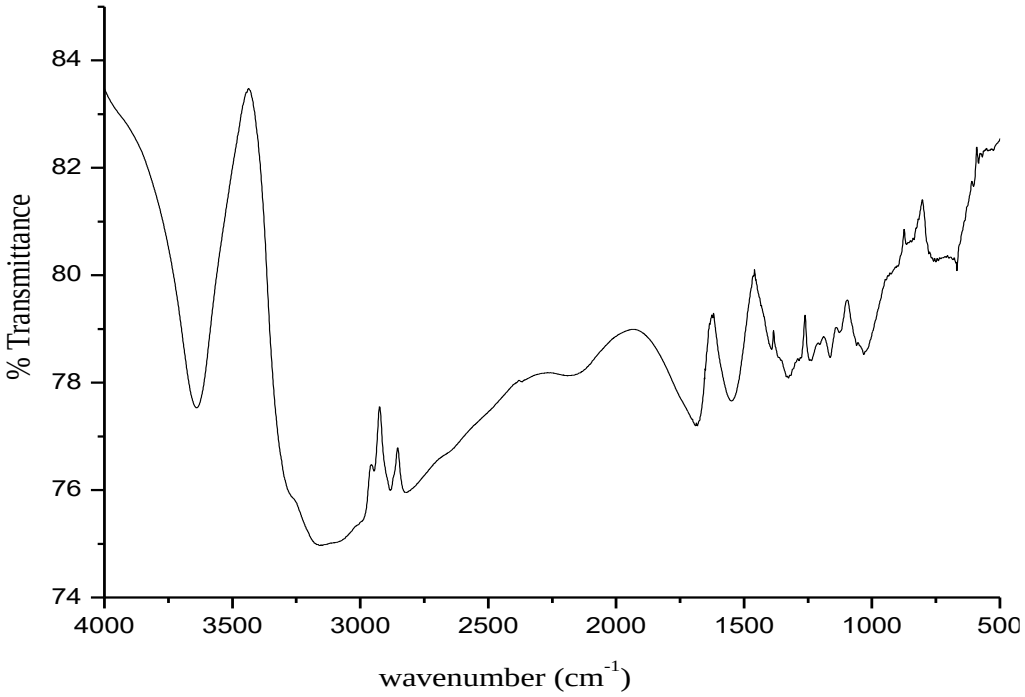

Figure 8. Fourier transform infrared (FTIR) spectrum of gelatin [50].

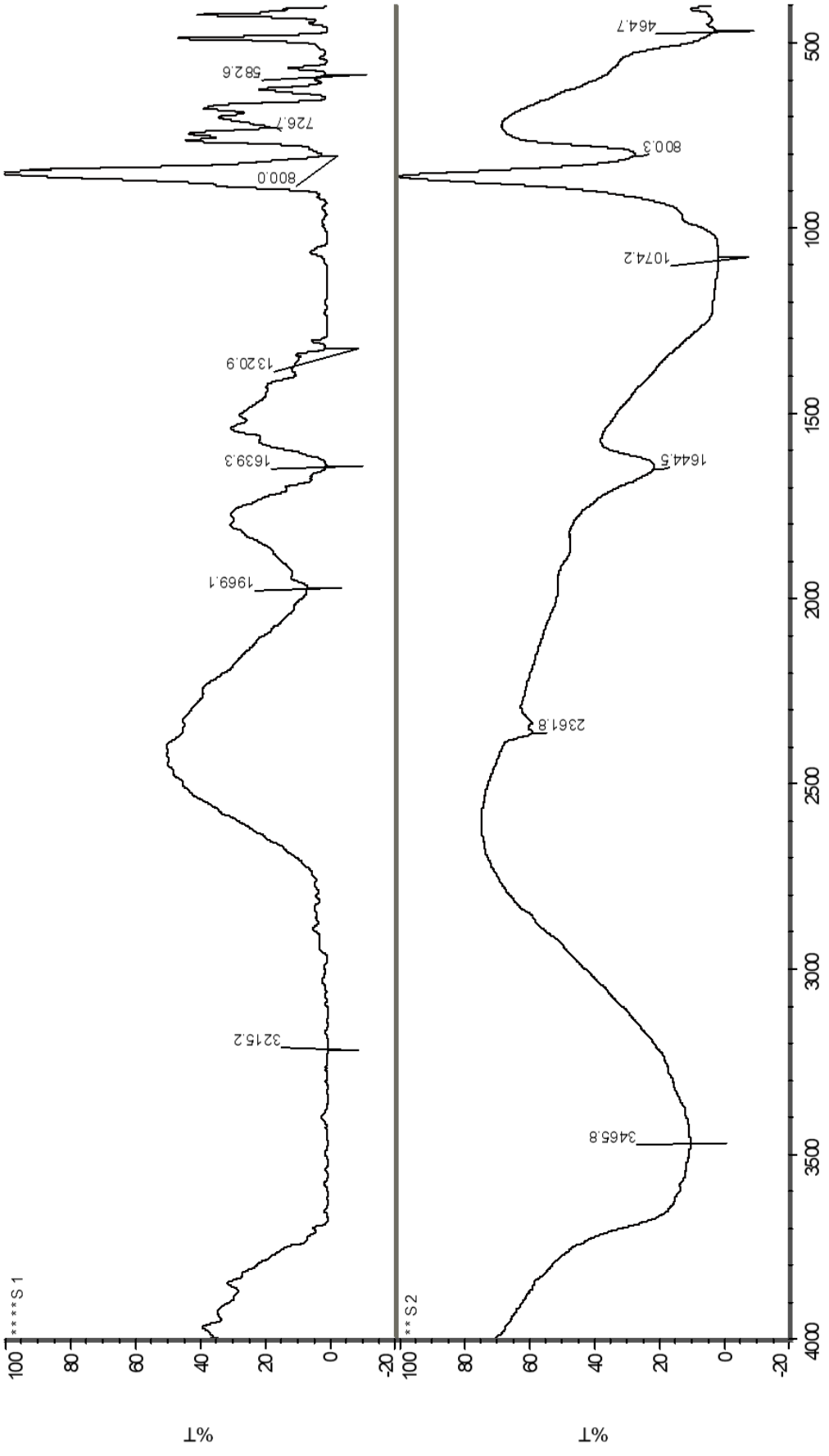

Figure 9. Fourier transform infrared (FTIR) spectrum of gelatin–silica hybrids (H_1 and H_{11}).

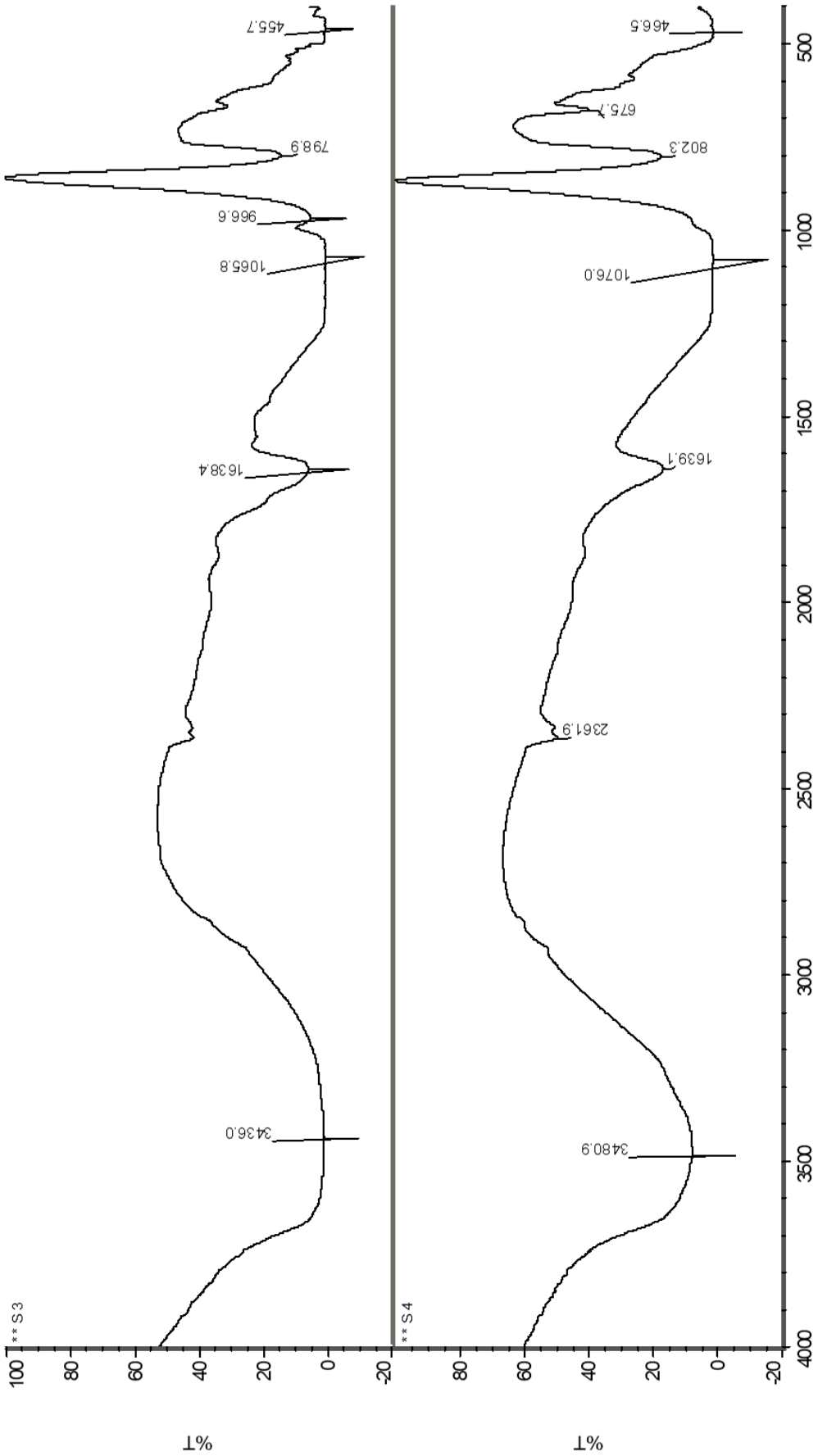

Figure 10. Fourier transform infrared (FTIR) spectrum of gelatin–silica (modified) hybrids (H_2 and H_{22}).

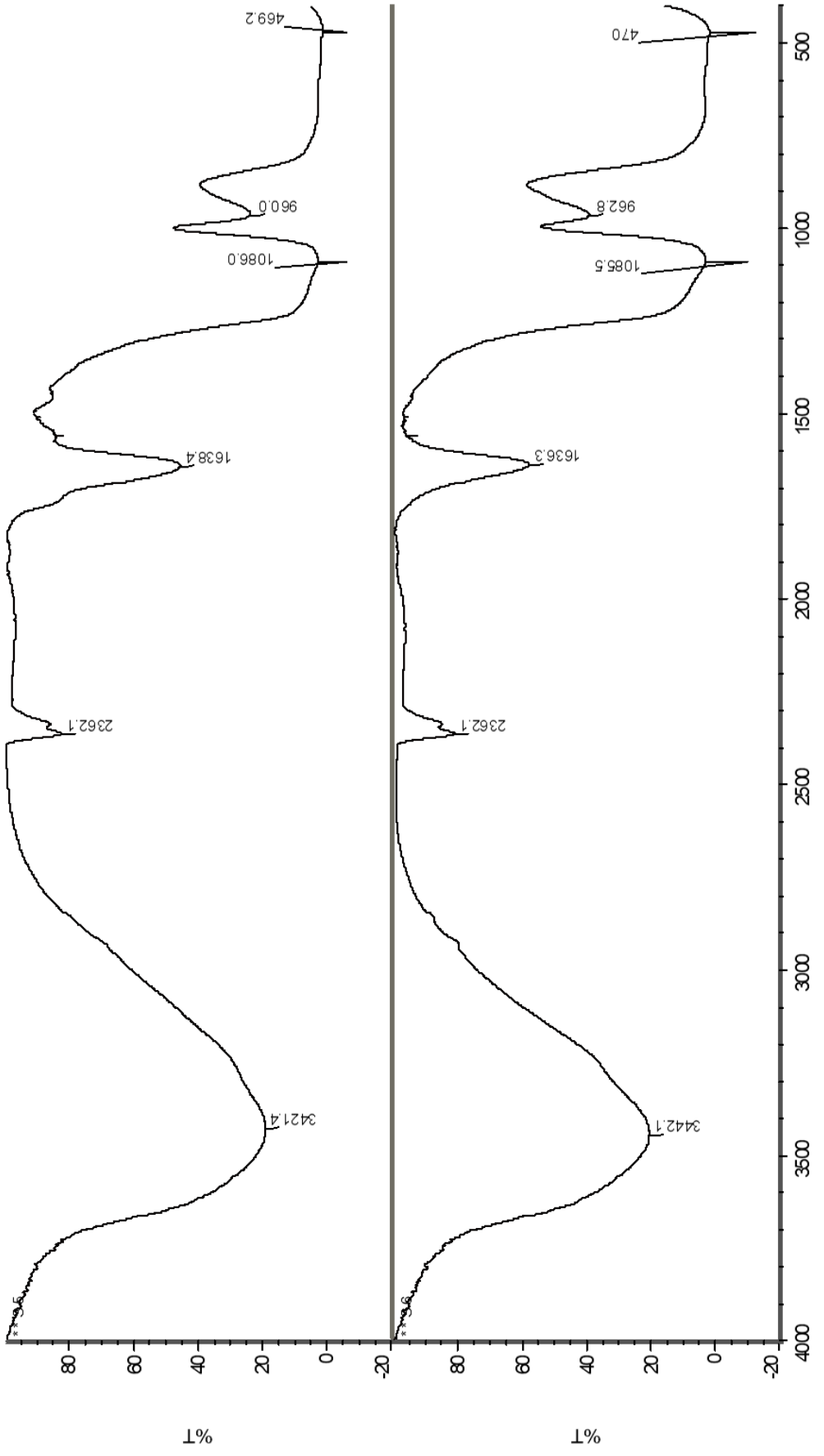

Figure 11. Fourier transform infrared (FTIR) spectrum of gelatin–titania hybrids (H_3 and H_{33}).

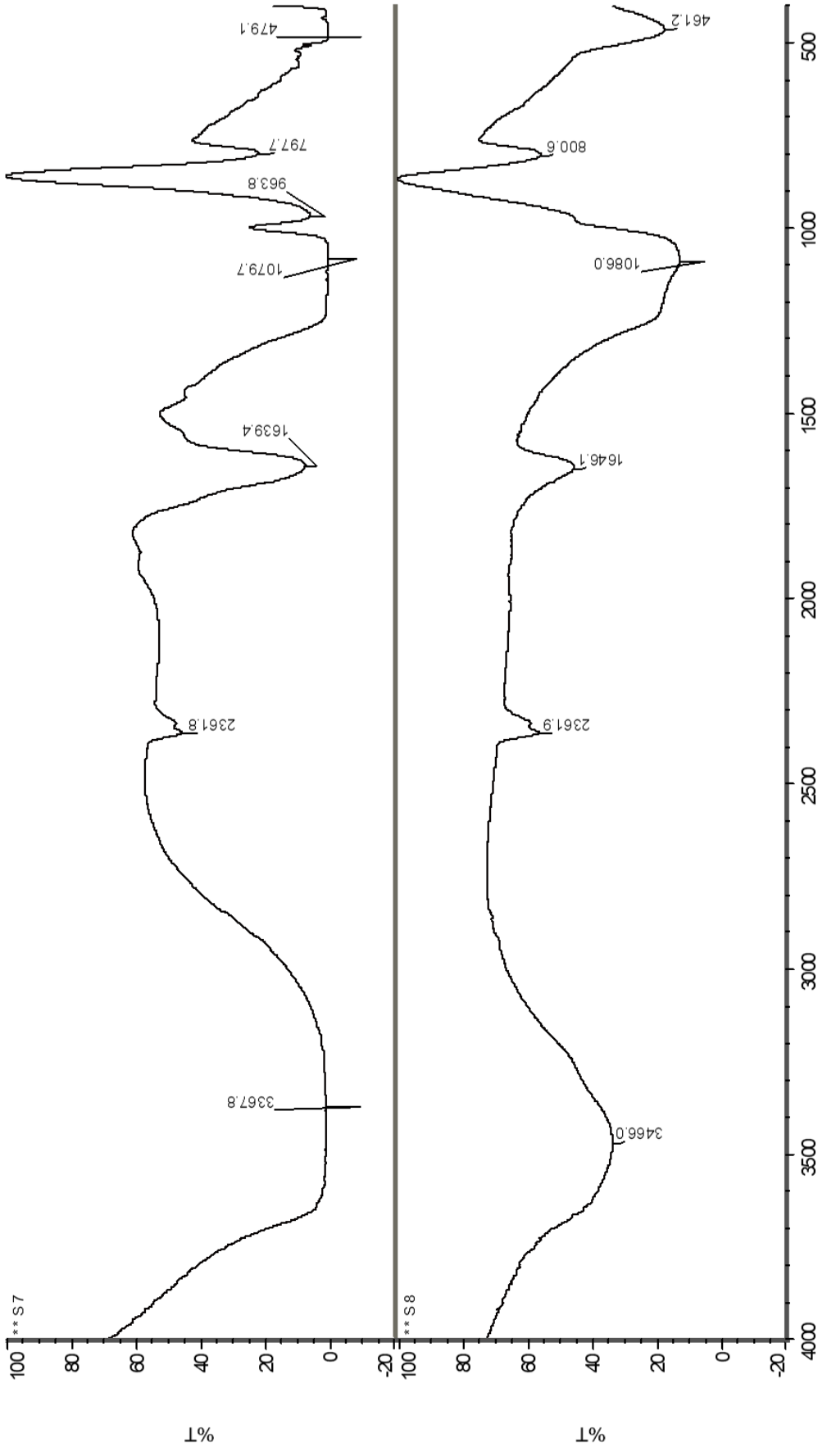

Figure 12. Fourier transform infrared (FTIR) spectrum of gelatin–zirconia hybrids (H_4 and H_{44}).

Thermogravimetric Analysis

Most researchers agree that TGA is the most useful technique for demonstrating the thermal stability of polymers across a broad temperature range. TGA of gelatin shows a weight loss in three distinct stages [45]. In first stage, gelatin shows about 9.49% loss in weight up to 100°C (Figure 13) which corresponds to the loss of adsorbed and bound water. In the second stage it shows 73.77% weight loss up to 400°C and that reflects the degradation of gelatin and evolution of volatile products resulting from its carbonization. In the third stage, carbonization formed at the second stage reduces by oxidation process and results in the loss of almost 88% up to 800°C. Synthesized hybrids are thermally more stable than that of gelatin (Table 2). First hybrid series resulted in 31.4% and 29.6% weight loss for H_1 and H_{11}, in which more than 15% loss is shown in the second stage up to 400°C as shown in Figure 14. Second hybrid series of modified gelatin–silica hybrid (H_2 and H_{22}) shows higher thermal stability as compared to gelatin and gelatin–silica hybrids (H_1 and H_{11}) with loss of only 21% for the as-synthesized and only 5% for the corresponding calcined from as presented in Figure 15. The presence of silica in the hybrid material makes them more hydrophobic. Similarly, Figure 16 and 17 show that the third (H_3 and H_{33}) and fourth (H_4 and H_{44}) hybrid series lost 25% and 19% weight up to 700°C, respectively.

Table 2. Thermogravimetric analysis (TGA) of hybrid materials at three different stages

Thermalgravimetric Analysis (% loss)						
S.N.	**Hybrid Material**		**100°C**	**400°C**	**>700°C**	**Total Loss**
1.	Gelatin–silica hybrid	H_1	6.1	16.2	9.1	31.4
2.		H_{11}	7.3	15.3	7.0	29.6
3.	Modified gelatin–silica hybrid	H_2	2.8	12.4	6.0	21.2
4.		H_{22}	2.7	1.9	0.1	4.7
5.	Modified gelatin–titania hybrid	H_3	4.7	14.4	5.2	24.3
6.		H_{33}	6.5	10.2	7.5	24.2
7.	Modified gelatin–zirconia hybrid	H_4	4.8	10.1	4.5	19.4
8.		H_{44}	5.1	9.4	4.3	18.8
9.	Gelatin		9.49	64.28	13.96	87.73

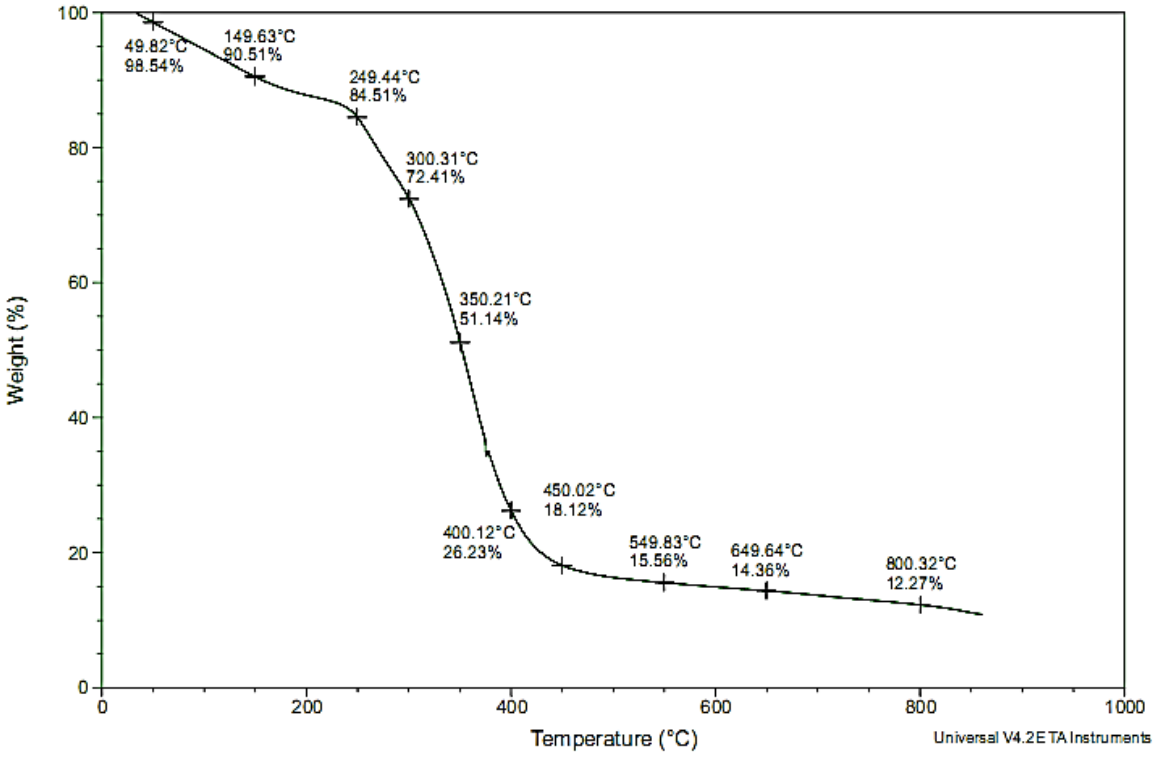

Figure 13. Thermogravimetric analysis (TGA) spectrum of gelatin [48].

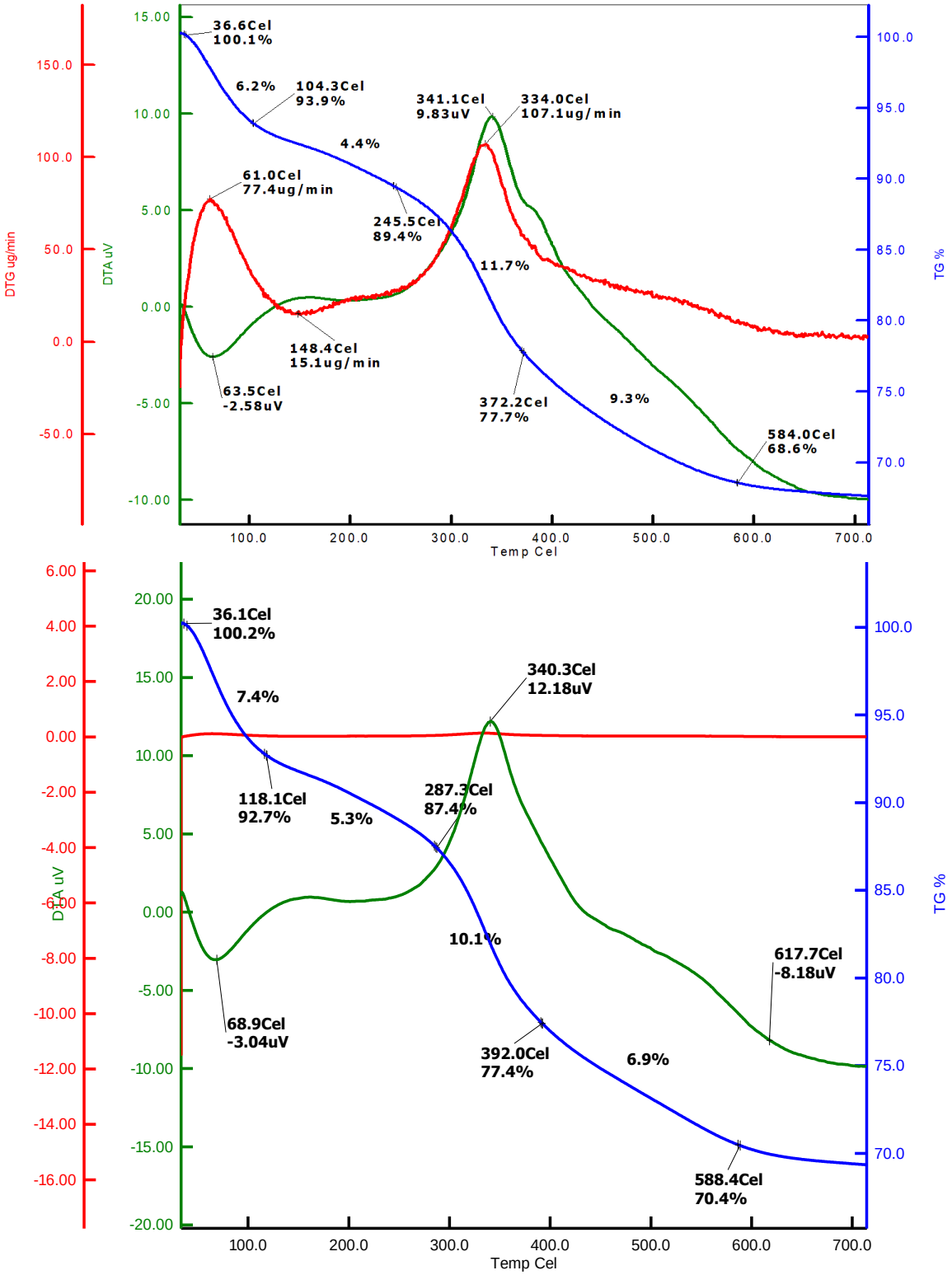

Figure 14. Thermogravimetric analysis (TGA) of gelatin–silica hybrids (H_1 and H_{11}).

It is the only free gelatin component or the unbound material that is mainly lost from the hybrids below 500°C. From 100°C to 500°C, the as-synthesized material lost more weight than that of the corresponding calcined material which may be due to the impurities present in addition to gelatin. These observations can be used as the guiding principle to synthesize tailored hybrid materials with well-controlled composition and the property profile.

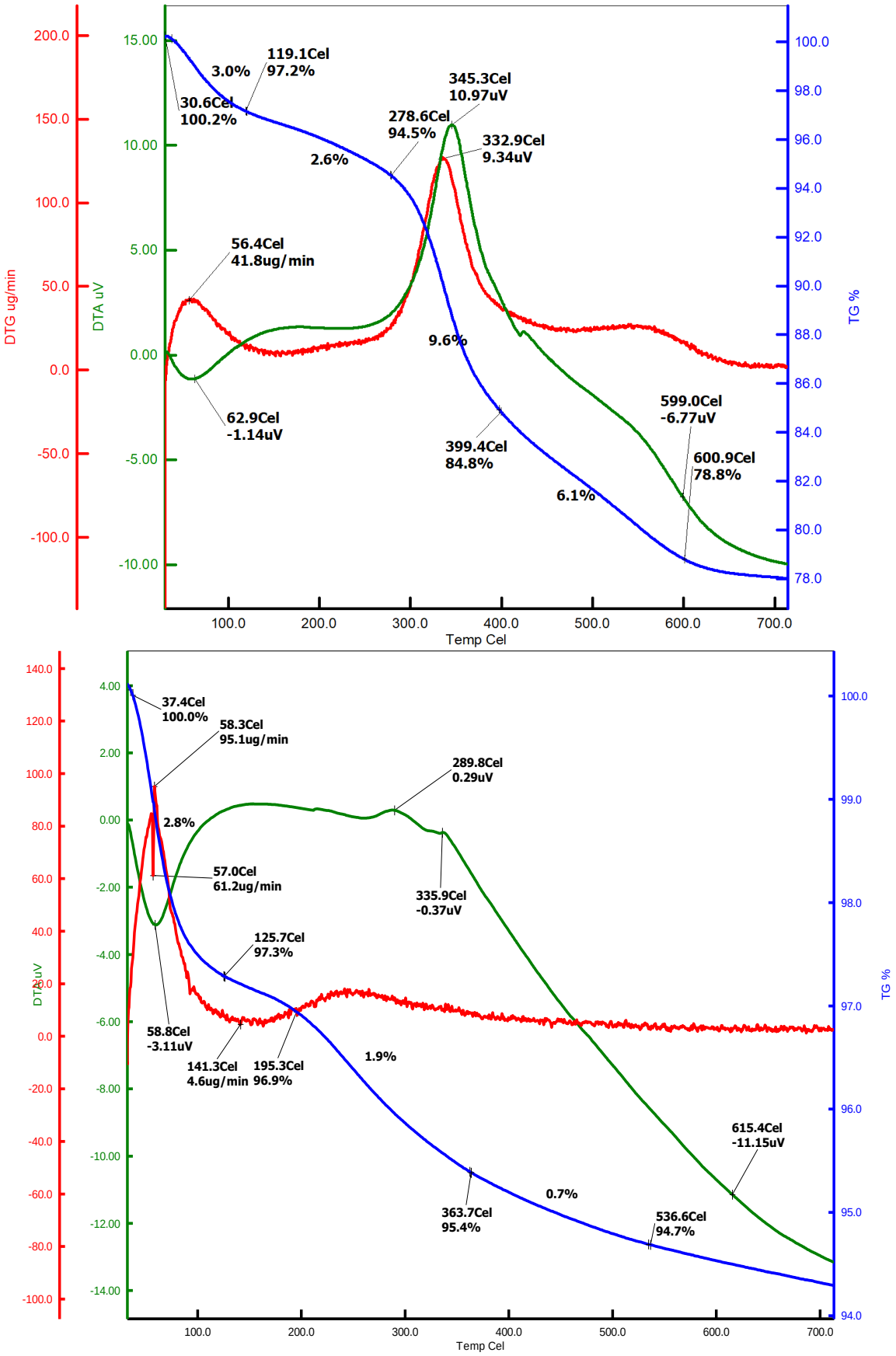

Figure 15. Thermogravimetric analysis (TGA) of modified gelatin–silica hybrids (H_2 and H_{22}).

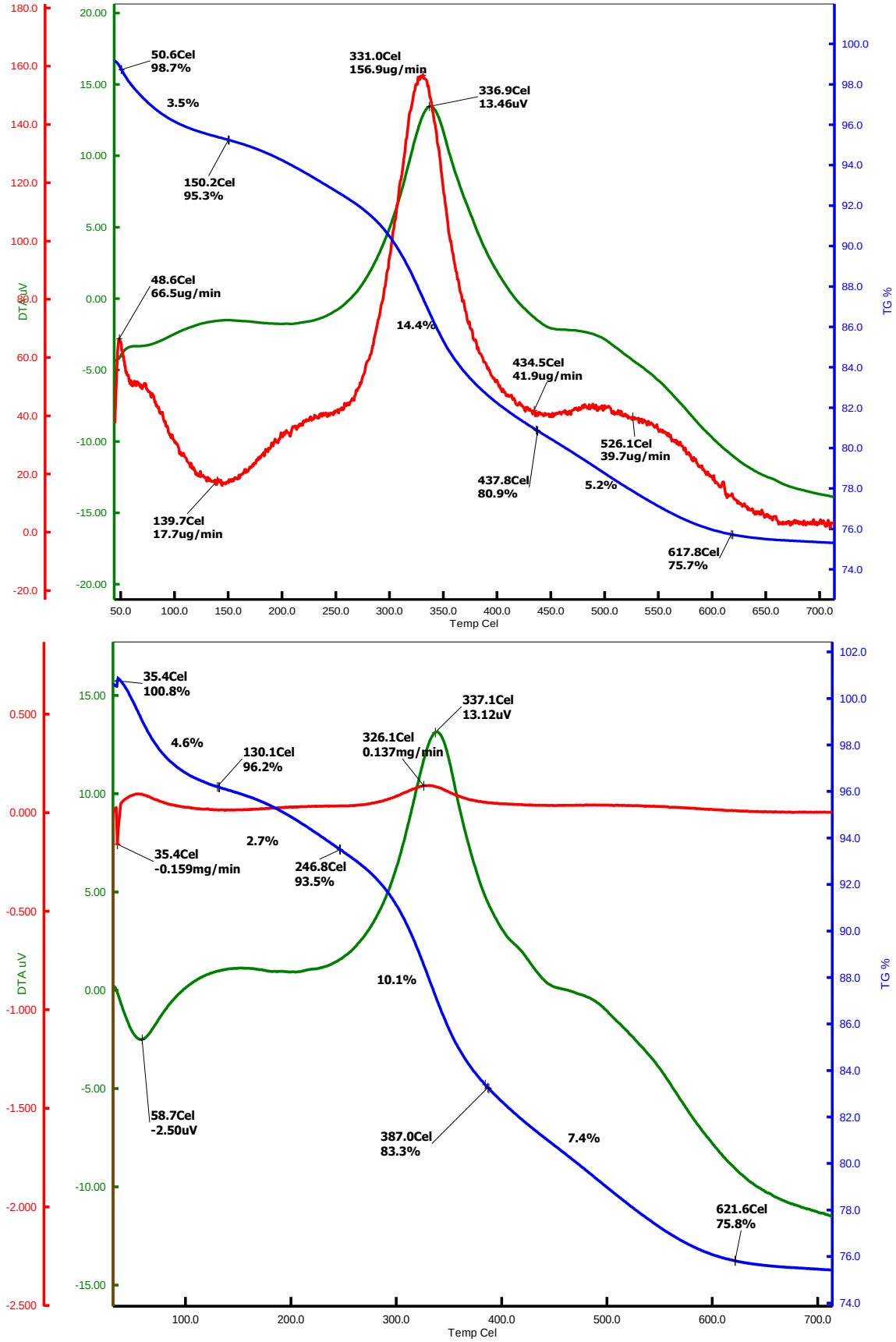

Figure 16. Thermogravimetric analysis (TGA) of gelatin–titania hybrid (H_3 and H_{33}).

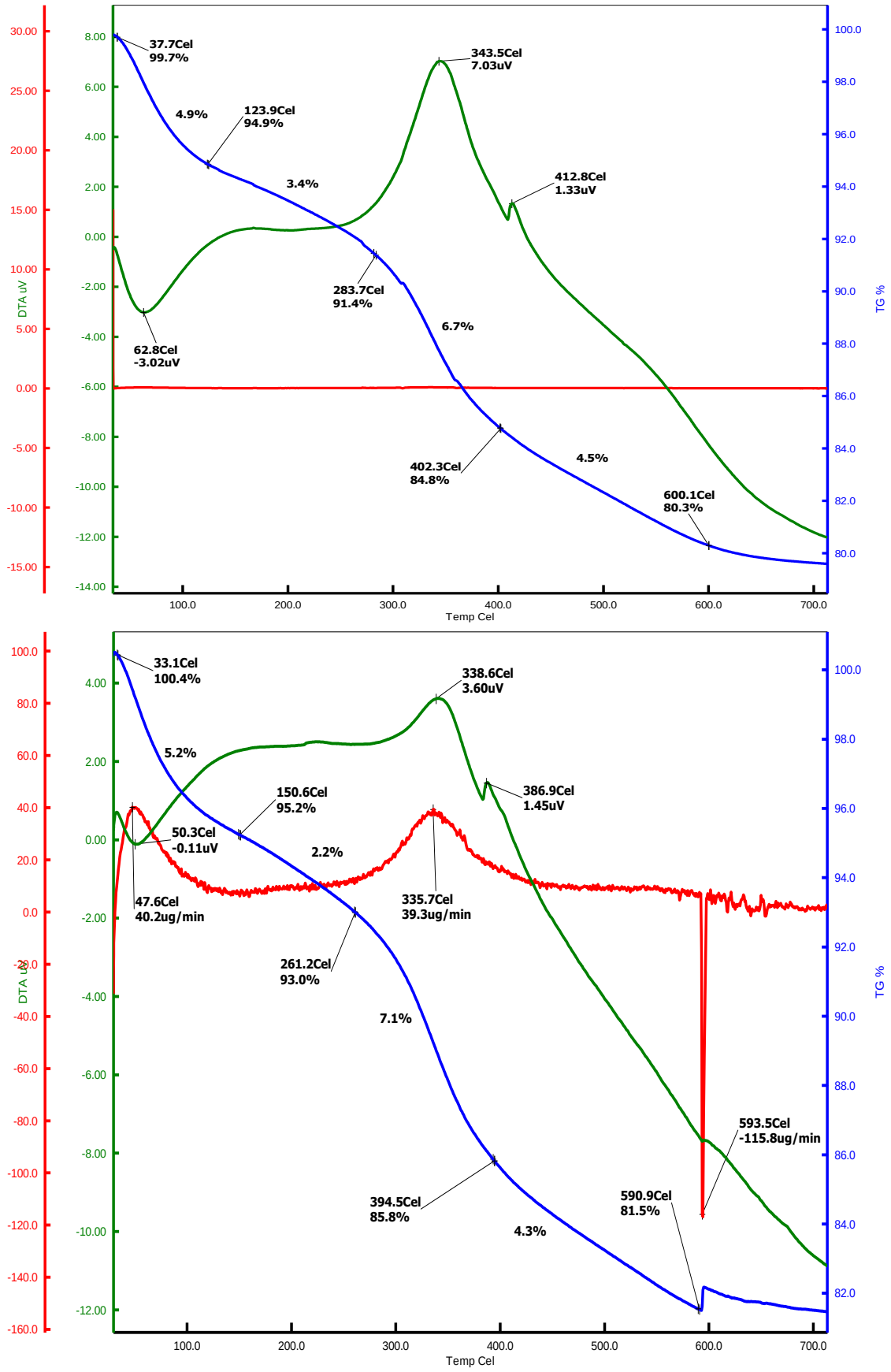

Figure 17. Thermogravimetric analysis (TGA) of gelatin–zirconia hybrids (H_4 and H_{44}).

These breakdown stages' appearance suggests that the structure of the gelatin chains has altered. Overall, the hybrid materials lost less weight than gelatin, indicating that gelatin's thermal stability was enhanced by hybrid formation. Compared to systems described by other authors, the hybrid system is more resistant to the breakdown of protein components [50].

X-Ray Diffraction Studies

Whether the material is crystalline or amorphous, XRD offers important insights into its structure and shape. Plotting powder diffraction patterns usually involves charting the angle (2θ) against the intensity of diffracted X-rays. When Bragg's law is followed, or when constructive interference is at its greatest, peaks in the diffraction pattern form at (2θ) values.

$$n\lambda = 2dsin\theta \quad (1)$$

The XRD spectra of different hybrid materials are presented in Figures 18 to 22. The XRD spectrum of gelatin with crystalline nature is shown in Figure 18. It has the peak intensity 288 at peak position 2θ (21.98°). The XRD spectra of the gelatin-silica hybrid are displayed in Figure 19, where the amorphous patterns of H_1 (as synthesized) and H_{11} (calcined) are nearly identical. Each diffraction peak has a broad peak of intensity, 422 and 382 at peak position 2θ (23.39° and 22.19°), with *d*-spacing (the distance between the diffracting planes) of 3.88 Å and 1.5747 Å. Finally, the intensities of the peaks are related to the types of atoms in the repeating planes, and the *d*-spacing of the observed peaks is related to the repeating distances between atom planes in the structure. XRD spectra of the modified gelatin–silica hybrid are as shown in Figure 20 with the peak intensities 502 and 746 at peak position 2θ (21.11° and 25.67°), where both materials of this hybrid series show crystalline nature as compared to the backbone gelatin and the first hybrid series. The calcined materials (H_{22}) are more crystalline than as-synthesized (H_2) but, have almost the same pattern. XRD spectra of modified gelatin–titania hybrid are shown in Figure 21, the intensity of the sharp peaks is 1609 and 2645 at peak position 2θ (25.34° and 25.37°) with most crystalline nature among all other hybrid series. Both the materials show exactly same XRD pattern, but the latter is more crystalline. Figure 22 shows the XRD spectra of modified gelatin–zirconia hybrid with the peak intensity of 309 and 763 at peak position 2θ (23.42° and 30.39°). The as-synthesized (H_4) material is more amorphous than calcined (H_{44}).

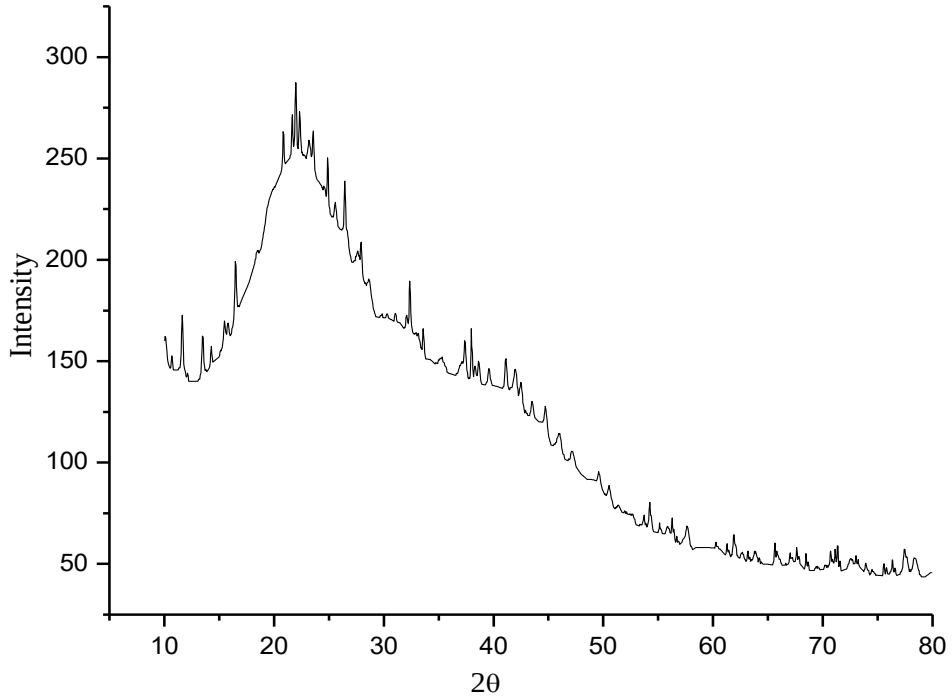

Figure 18. X-ray diffraction (XRD) spectrum of gelatin.

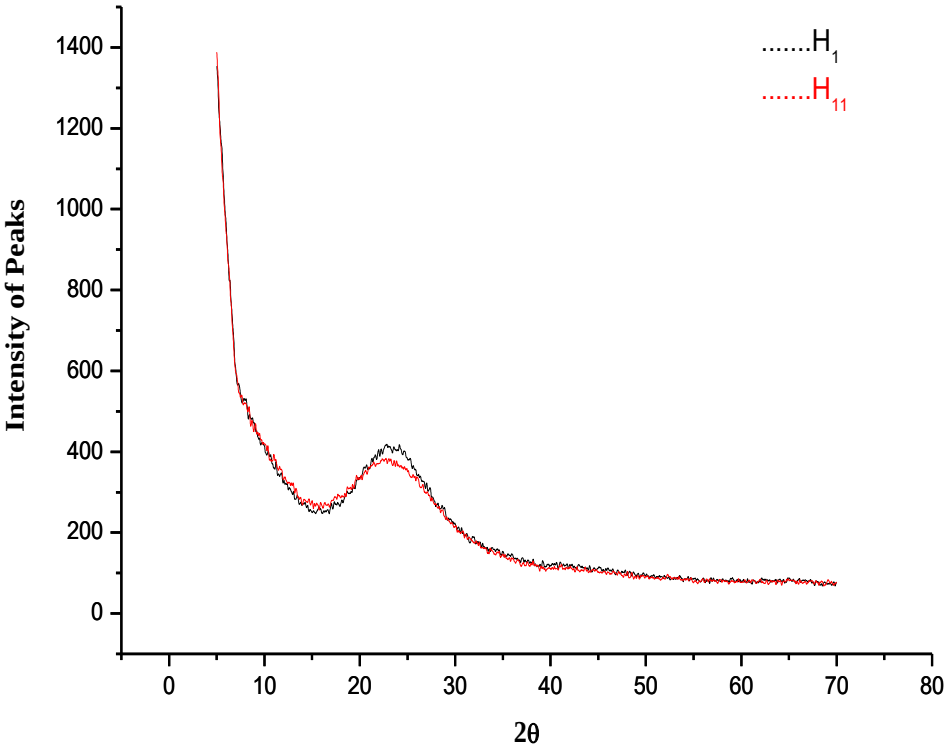

Figure 19. X-ray diffraction (XRD) spectra of gelatin–silica hybrids (H_1 and H_{11}).

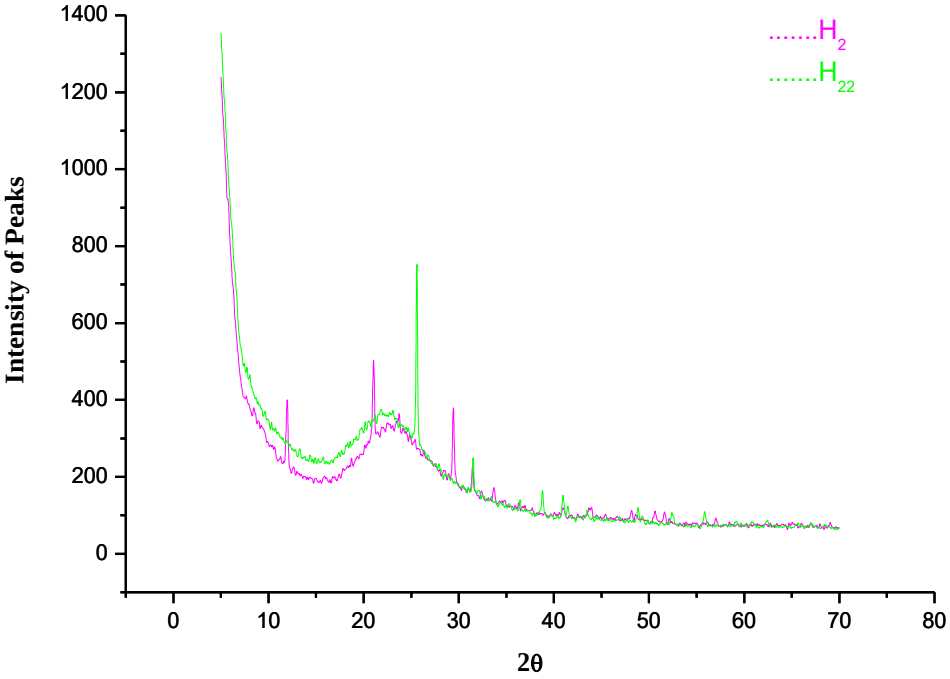

Figure 20. X-ray diffraction (XRD) spectra of modified gelatin–silica hybrids (H_2 and H_{22}).

From XRD spectra of the hybrid materials, it can be observed that backbone structure opens up due to the modification and hence affects the crystallinity, thereby making the hybrids more amorphous in nature except third hybrid series (modified gelatin–titania hybrid) which was observed to be crystalline in nature with most intense peaks. This might be due to the fact that with an increase in the cross-linker (TEOS) concentration, cross-linking density between the biopolymeric backbone get enhanced leading to more alignment of the biopolymer chains and consequent crystalline structure.

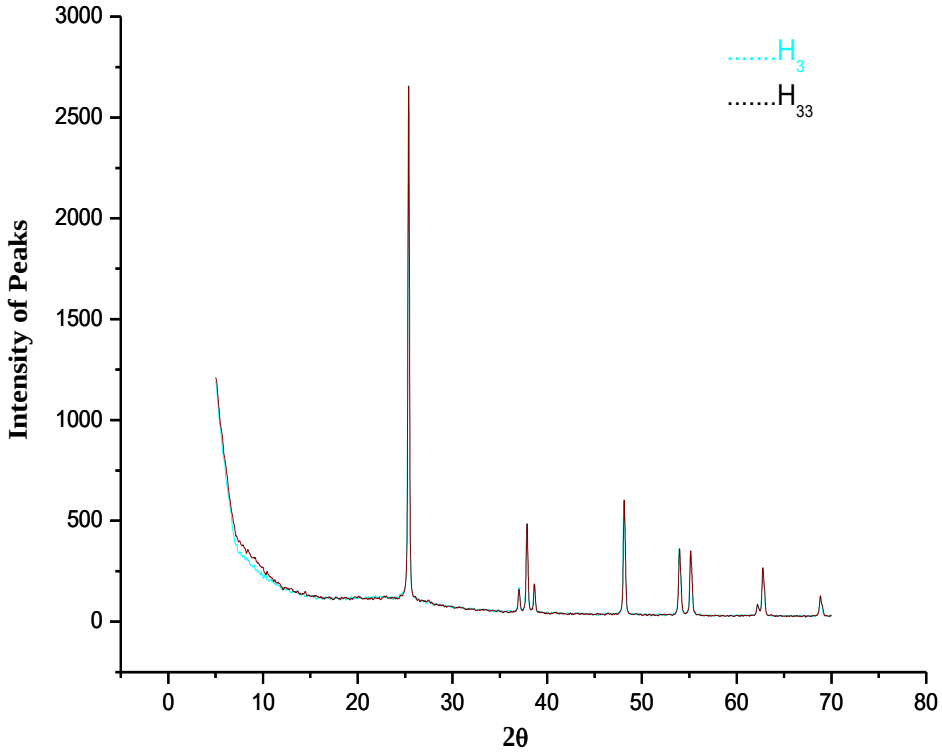

Figure 21. X-ray diffraction (XRD) spectra of gelatin–titania hybrids (H_3 and H_{33}).

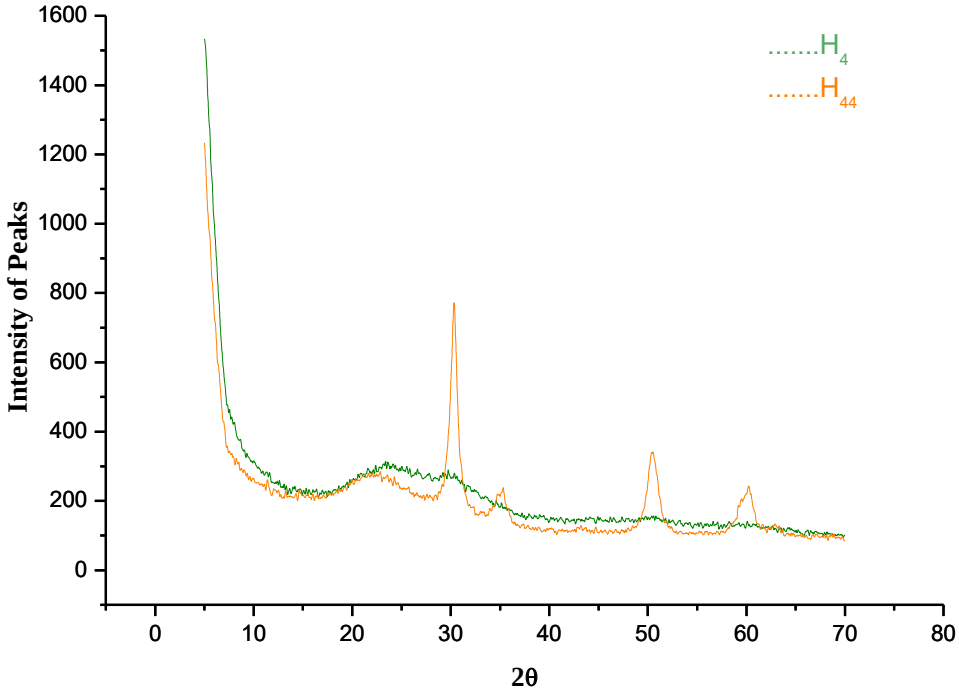

Figure 22. X-ray diffraction (XRD) spectrum of gelatin–zirconia hybrids (H_4 and H_{44}).

The crystallite size of the hybrid materials was calculated using the Scherer formula given by Equation (2). The wavelength of the source was 1.5406 Å for all the XRD studies recorded. The crystallite size for all the four hybrids comes out to be less than a nanometer (<1 nm) the data is shown in Table 3.

$$D_p = \frac{0.94}{\beta_{1/2} cos\theta} \lambda \quad (2)$$

Table 3. Crystallite size calculations using Scherrer Formula from X-ray diffraction (XRD) studies.

S.N.	Peak FWHM$\beta_{1/2}$ (degrees)	Peak Position 2θ (degrees)	Crystallite Size (nm)	Lattice Strain
H_1	23.115	23.39	0.370	0.4872
H_{11}	22.75	22.19	0.370	0.5062
H_2	22.327	21.109	0.380	0.5229
H_{22}	25.272	25.666	0.339	0.4841
H_3	25.356	25.345	0.339	0.4920
H_{33}	25.383	25.374	0.339	0.4920
H_4	23.748	23.426	0.360	0.4998
H_{44}	30.318	30.389	0.279	0.4871

FWHM, full-width at half-maximum.

Scanning Electron Microscopy–Energy Dispersive X-Ray Spectroscopy Studies

One of the most important properties that must be considered in the characterization of the hybrid materials is their mesoporous morphologies. Surface morphology of a polymeric hybrid material network depends upon various factors like conditions followed during the synthesis, amount and nature of cross-linker or silylation material (TEOS), medium of the sol–gel process, solvent system used and calcination process. The surface morphologies of these nano-hybrids were compared from their scanning electron micrographs (SEMs) images taken at different magnification power. The polymer backbone monomer structure and reaction conditions affect the surface morphology of the hybrid materials. At the higher magnification pores are clearly visible on the surface of the networks. In the present case the SEM images of gelatin–silica, modified gelatin–silica, gelatin–titania, and gelatin–zirconia hybrid materials at comparable magnifications are presented in Figures 23 to 26. The hybrid materials form agglomerates which are mesoporous. These agglomerates show rough and interconnected porous surface. It is proposed that the interconnected, porous, rough surface and the flexibility of the hybrid material makes it suitable for the removal of toxic metal ions, organic dyes, drug delivery devices and for the enzyme immobilization processes. The agglomeration of the nano-hybrids may be due to surfactant (SDS) during sol–gel process. Differences in the morphological behavior and porous nature of the hybrid materials surface are clearly visible in the SEMs.

The gelatin–silica, modified gelatin–silica hybrid materials exhibit more open network with high surface area but less mesoporous than those of gelatin–titania, and gelatin–zirconia hybrids. While in the latter case, more intense pores of smaller size are present due to the interactions or association of the titania and zirconia with gelatin backbone. The morphology of all the hybrid series has been found to be slightly different from the other micrographs due to the variation of the hydrophilic groups in the resulting TEOS cross-linked hybrid materials. Thus, it confirms that the changes affected in the surface morphology after sol–gel reactions. It is clearly established from the SEM study of the gelatin-based hybrid materials that the synthesized materials in the present work have a mesoporous structure. The pore size increased for the calcined materials as compared to the as-synthesized hybrid materials which can be credited to water evaporation resulting during the calcination process. These pores are believed to be the regions of water or other unstable molecules for penetration. These are also supposed to be interactional sites for external stimuli with the hydrophilic groups of the resulting nano-hybrids. Thus, porosity plays an important role to enhance the total water sorption capability and the rate of response by reducing the transport resistance. Therefore, mesoporous hybrid materials have been considered as versatile process material in many ways.

The samples were analyzed for elemental content of oxygen, silicone, titanium, and zirconium as per hybrid composition using SEM−EDX studies. The EDS/EDX spectra produced are shown in Figures 27 to 30 and the raw data of the percentage composition by weight and percentage atom of these elements is shown in Tables 4 to 7. It is clear from the analysis that the O, Si, Ti, and Zr are present in the gelatin–silica, modified gelatin–silica, gelatin–titania, and gelatin–zirconia hybrid materials.

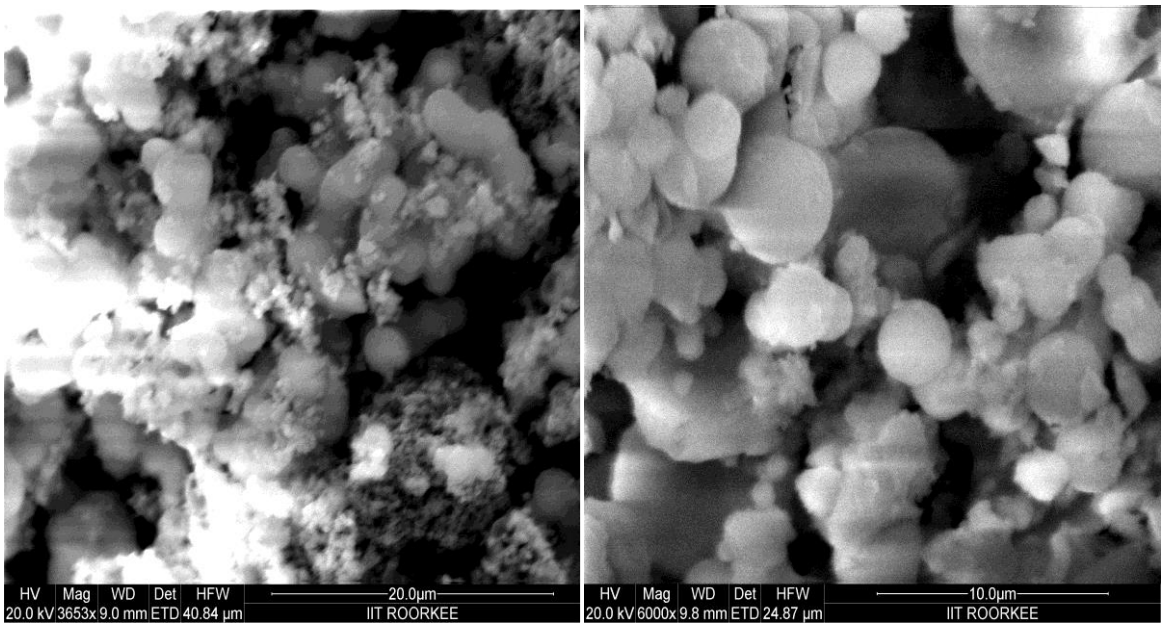

Figure 23. Scanning electron microscopy (SEM) images of H_1 and H_{11}.

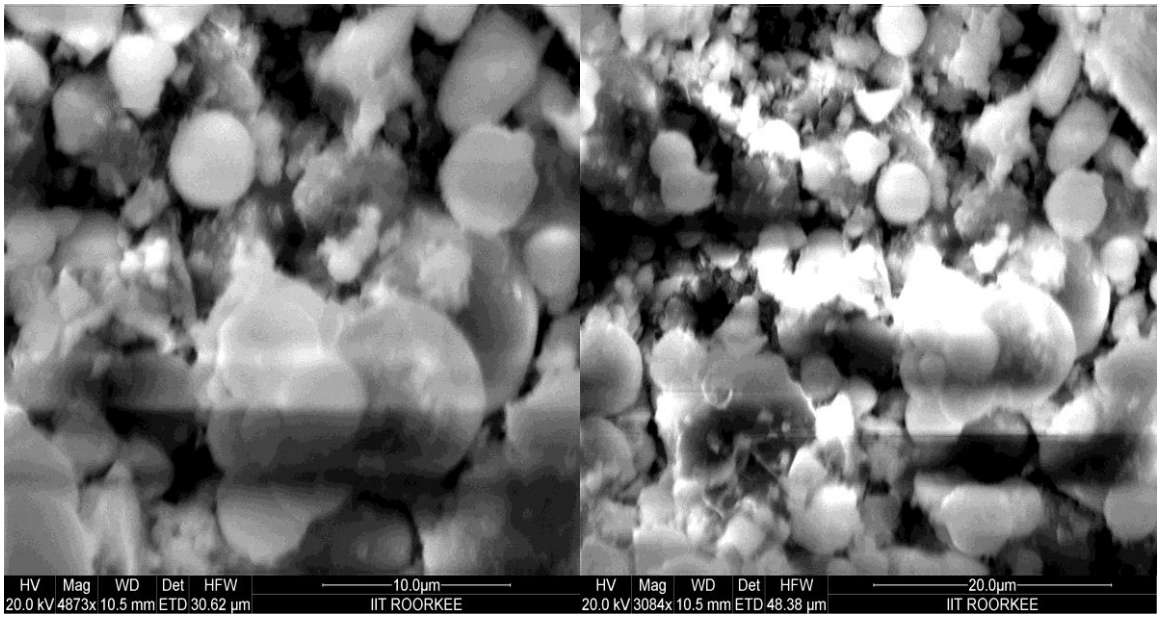

Figure 24. Scanning electron microscopy (SEM) images of H_2 and H_{22}.

Table 4. Compositional analysis data for first hybrid series (H_1 and H_{11}).

Hybrid Material	EI	AN	Series	unn. C [wt. %]	nor. C [wt. %]	Atom. C [wt. %]	Error [wt. %]
H_1	O	8	K–Series	62.10	66.93	78.04	8.5
	Si	14	K–Series	30.68	33.07	21.96	1.4
	Total			92.78	100.00	100.00	
H_{11}	O	8	K–Series	61.50	67.59	78.54	8.8
	Si	14	K–Series	29.49	32.41	21.46	1.3
	Total			90.98	100.00	100.00	

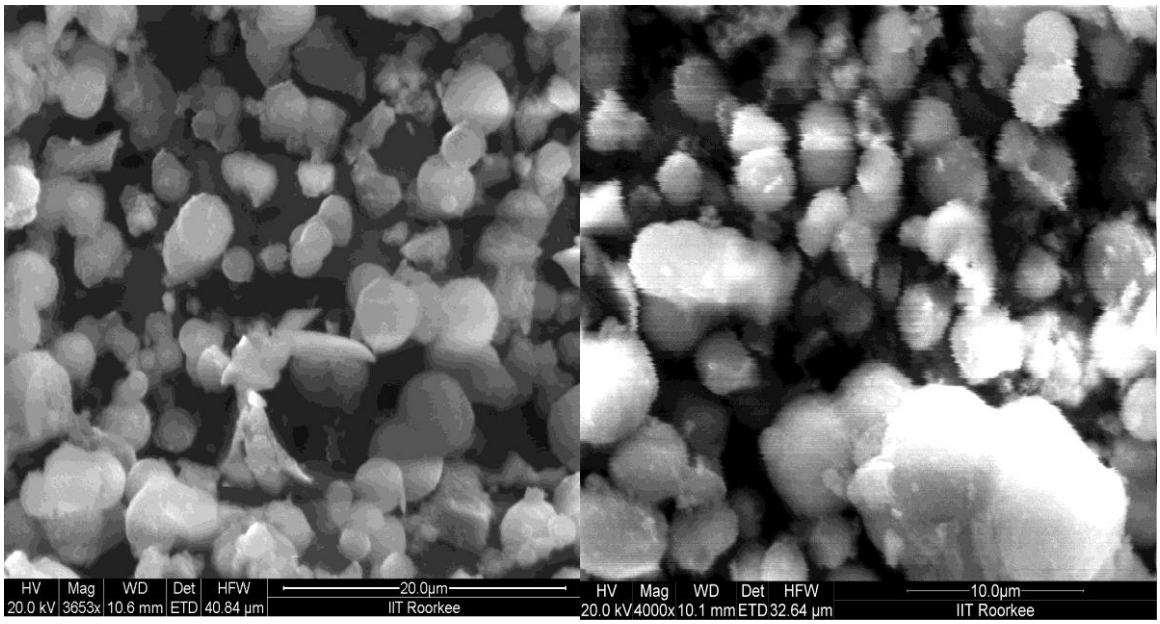

Figure 25. Scanning electron microscopy (SEM) images of H_3 and H_{33}.

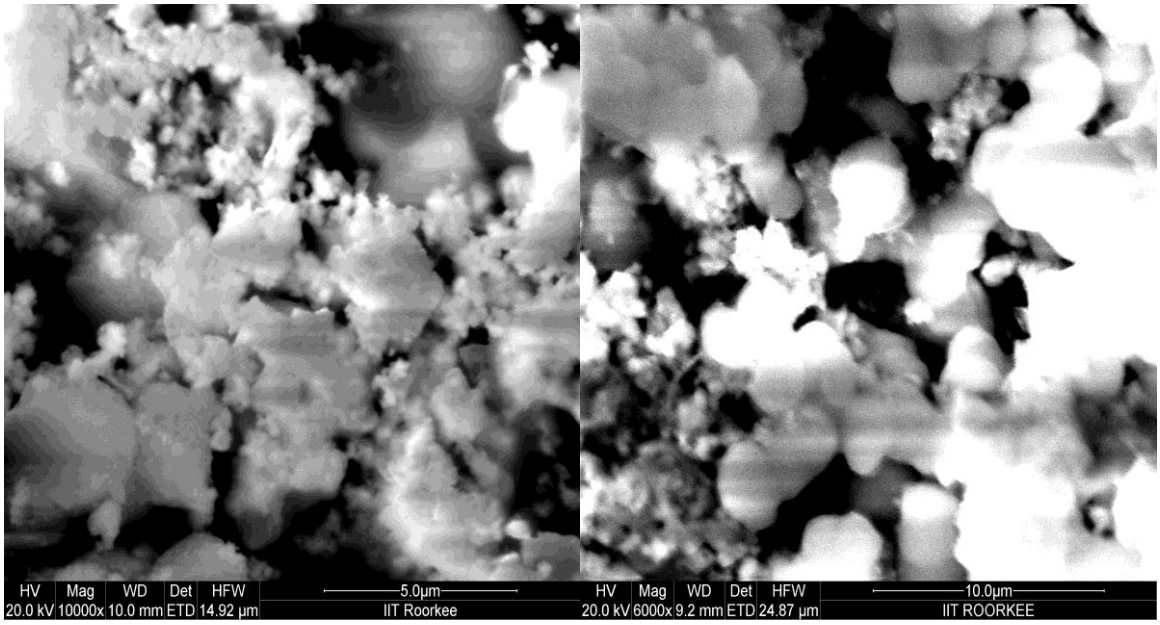

Figure 26. Scanning electron microscopy (SEM) images of H_4 and H_{44}.

Table 5. Compositional analysis data for second hybrid series (H_2 and H_{22})

Hybrid Material	EI	AN	Series	unn. C [wt. %]	nor. C [wt. %]	Atom. C [wt. %]	Error [wt. %]
H_2	O	8	K–Series	57.96	65.84	77.18	7.5
	Si	14	K–Series	30.08	34.16	22.82	1.3
	Total			88.04	100.00	100.00	
H_{22}	O	8	K–Series	53.74	68.17	78.99	8.7
	Si	14	K–Series	25.09	31.83	21.01	1.1
	Total			78.83	100.00	100.00	

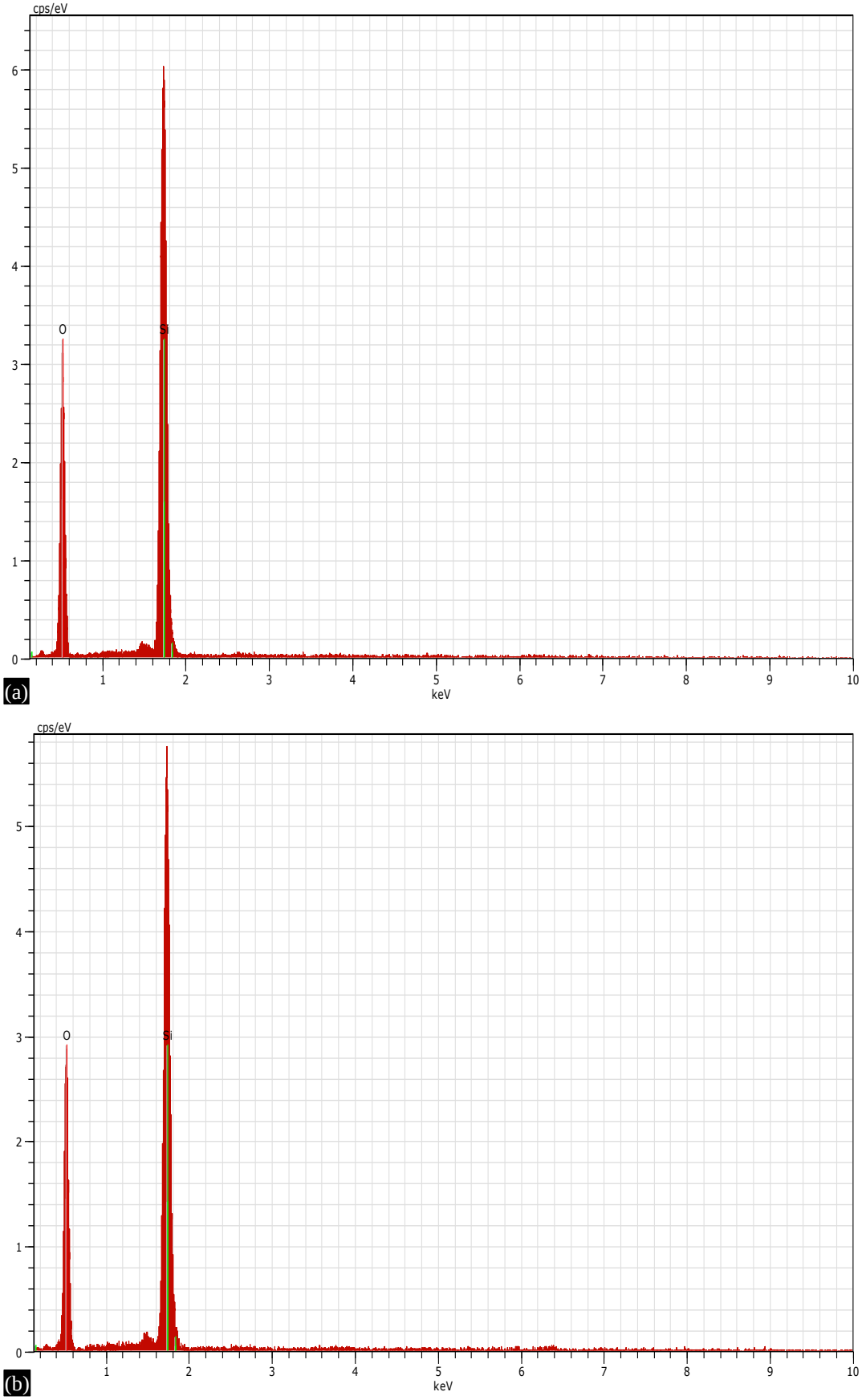

Figure 27. (a and b) Energy dispersive X-ray spectroscopy (EDS) spectrum: H_1 and H_{11}.

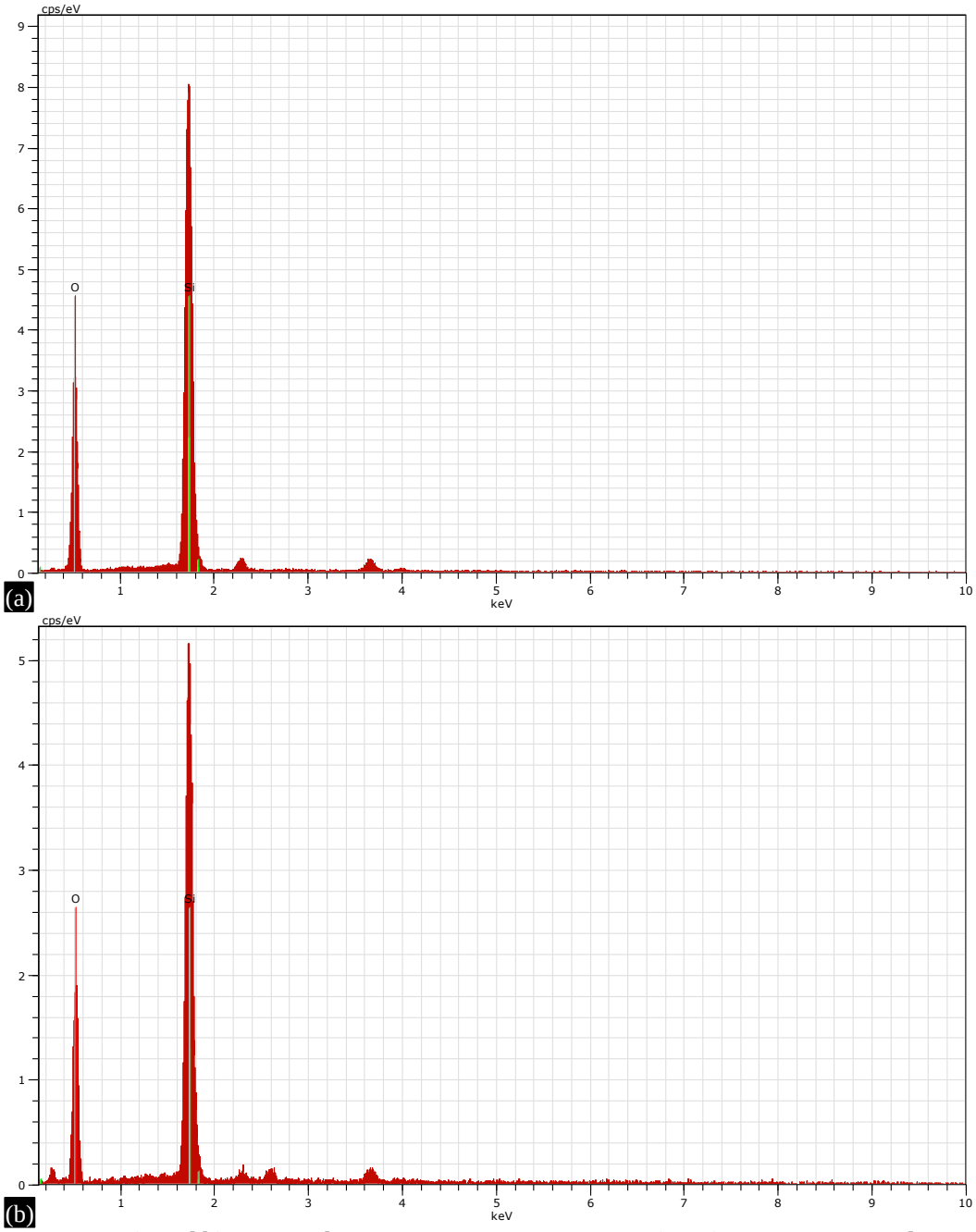

Figure 28. (a and b) Energy dispersive X-ray spectroscopy (EDS) spectrum: H_2 and H_{22}.

Table 6. Compositional analysis data for third hybrid series (H_3 and H_{33})

Hybrid Material	EI	AN	Series	unn. C [wt. %]	nor. C [wt. %]	Atom. C [wt. %]	Error [wt. %]
H_3	O	8	K–Series	47.03	47.71	69.16	50.7
	Ti	22	K–Series	36.38	36.14	17.51	1.1
	Si	14	K–Series	16.25	16.14	13.33	0.7
	Total			100.66	100.00	100.00	
H_{33}	O	8	K–Series	50.44	50.69	71.04	43.5
	Ti	22	K–Series	31.41	31.56	14.78	0.9
	Si	14	K–Series	17.66	17.75	14.17	0.8
	Total			99.51	100.00	100.00	

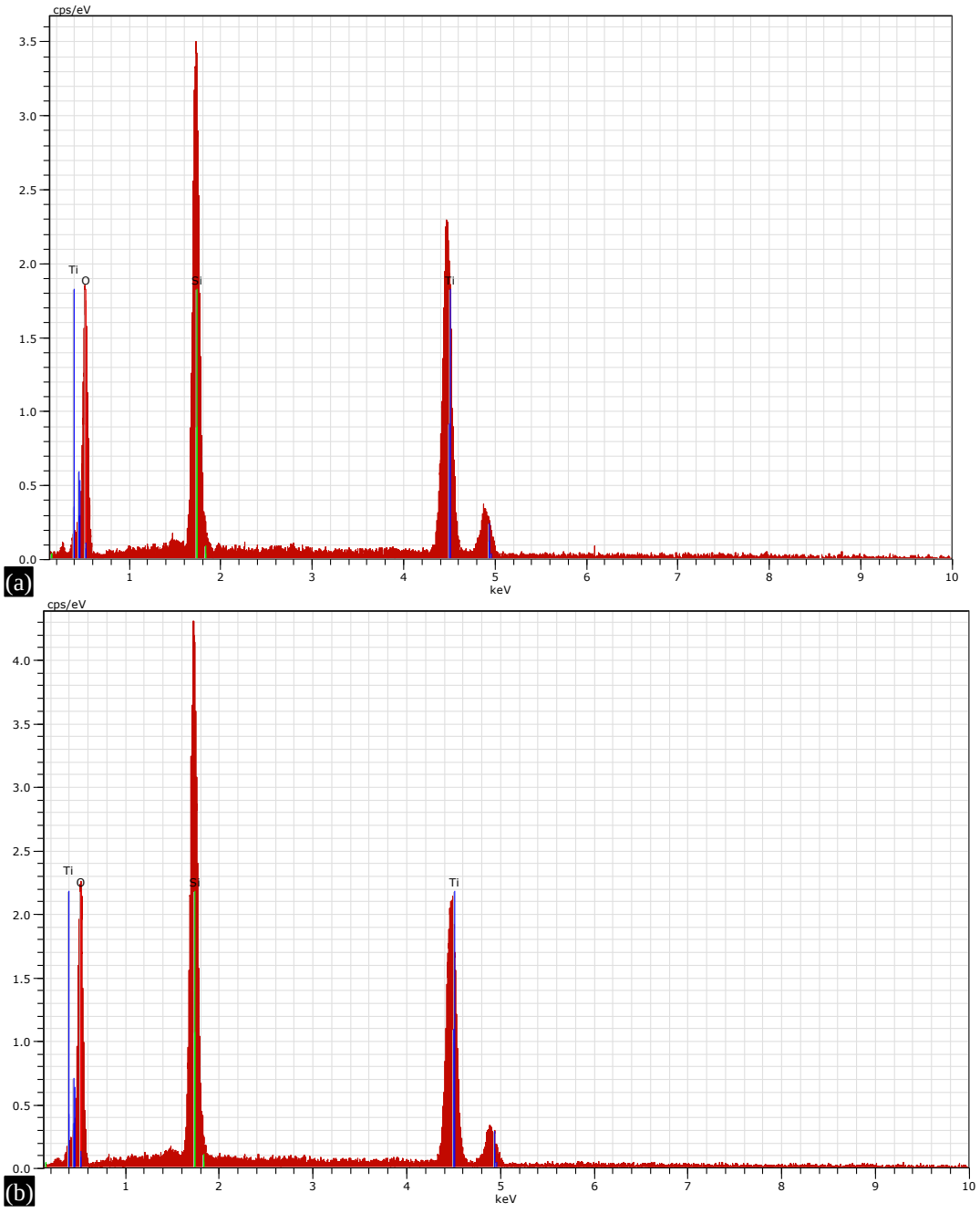

Figure 29. (a and b)Energy dispersive X-ray spectroscopy (EDS) spectrum: H_3 and H_{33}.

Table 7. Compositional analysis data for fourth hybrid series (H_4 and H_{44}).

Hybrid Material	EI	AN	Series	unn. C [wt. %]	nor. C [wt. %]	Atom. C [wt. %]	Error [wt. %]
H_4	O	8	K–Series	55.12	64.22	78.66	7.9
	Si	14	K–Series	24.27	28.28	19.73	1.1
	Zr	40	L–Series	6.44	7.50	1.61	0.4
	Total			85.83	100.00	100.00	
H_{44}	O	8	K–Series	55.14	63.04	77.15	7.0
	Si	14	K–Series	27.04	30.92	21.55	1.2
	Zr	40	L–Series	5.29	6.05	1.30	0.3
	Total			87.47	100.00	100.00	

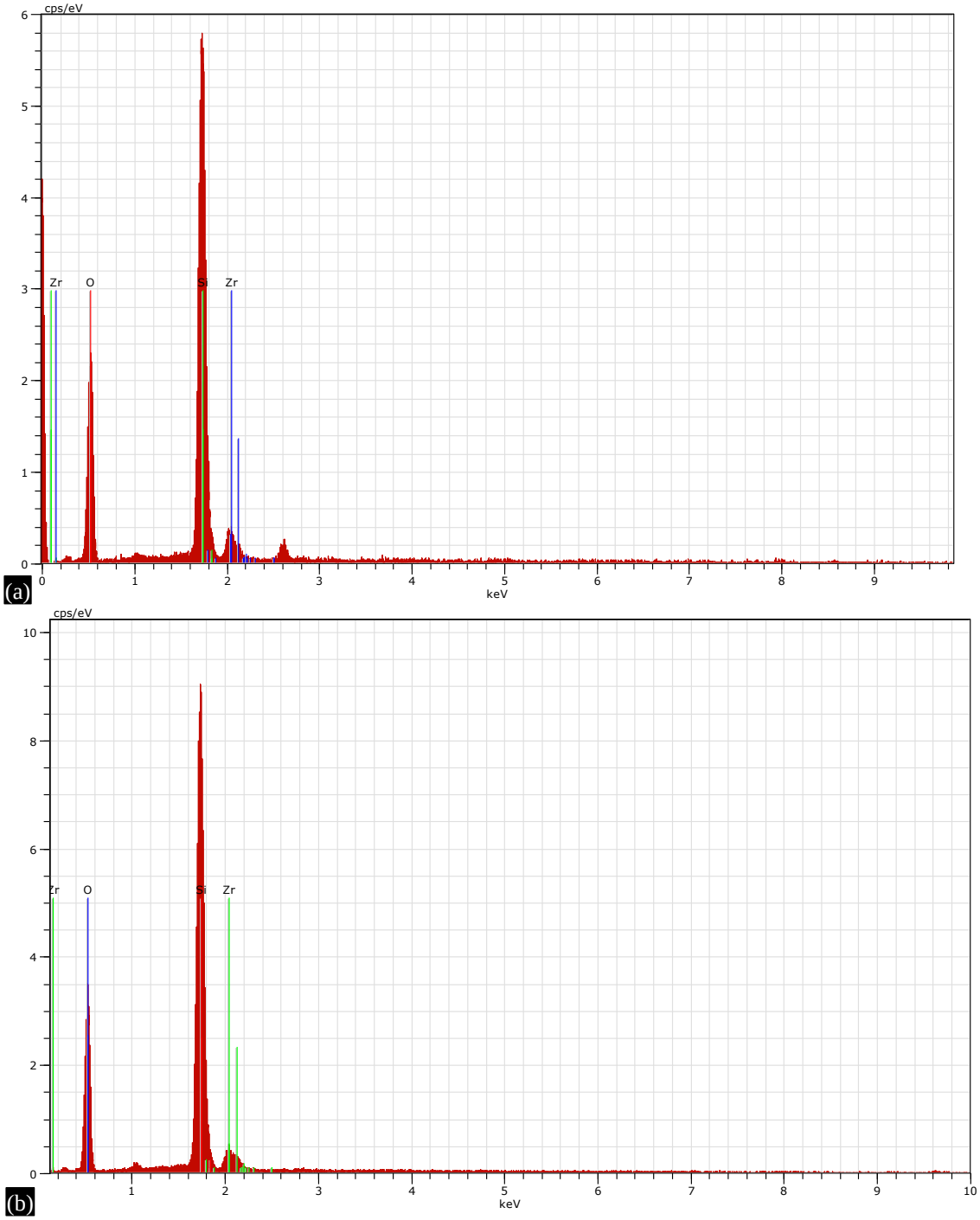

Figure 30. (a and b) Energy dispersive X-ray spectroscopy (EDS) spectrum: H_4 and H_{44}.

The data presented in Tables 4 to 7 show large amounts of silicon and oxygen as compared to other elements that most likely originate from the glass substrate used during the instrumentation. Since in EDS/EDX, the majority of x-ray excitation originates from a volume under the surface of almost 1µm diameter, therefore it is expected that most of the x-rays detected would be from the underlying glass substrate used for EDS/EDX analysis [49].

Transmission Electron Microscopy Studies

TEM images of the gelatin–silica, modified gelatin–silica, gelatin–titania, and gelatin–zirconia hybrids were carried out to determine the morphology and size of the synthesized hybrid materials. The

TEM results indicated that size of the materials is in the range 80 to 120 nm (Figures 31–35). As compared to SEM images the TEM images give a better indication of the particle size as each particle is dispersed and can be seen separately. It provides the internal structure morphology of the materials.

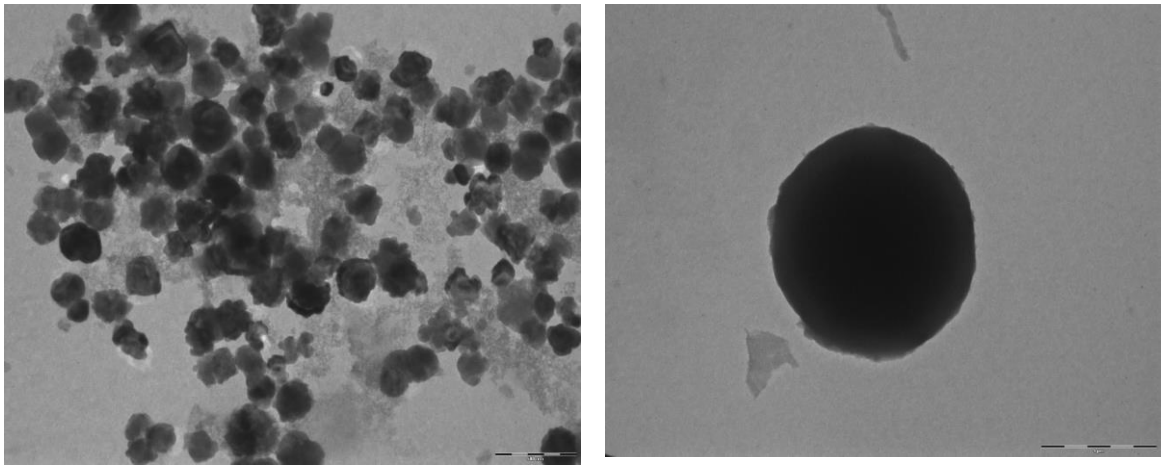

Figure 31. Transmission electron microscopy (TEM) image of H_1 and H_{11}.

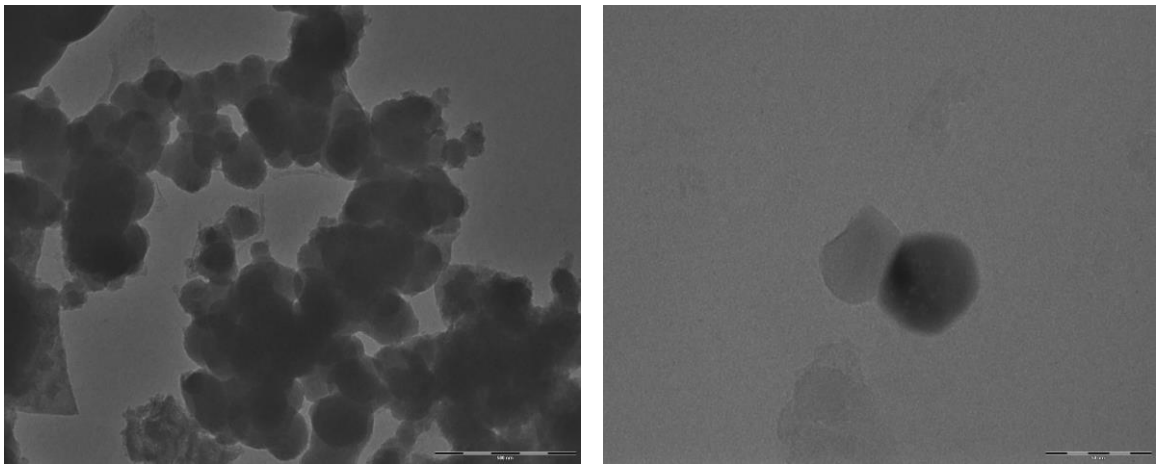

Figure 32. Transmission electron microscopy (TEM) image of H_2 and H_{22}

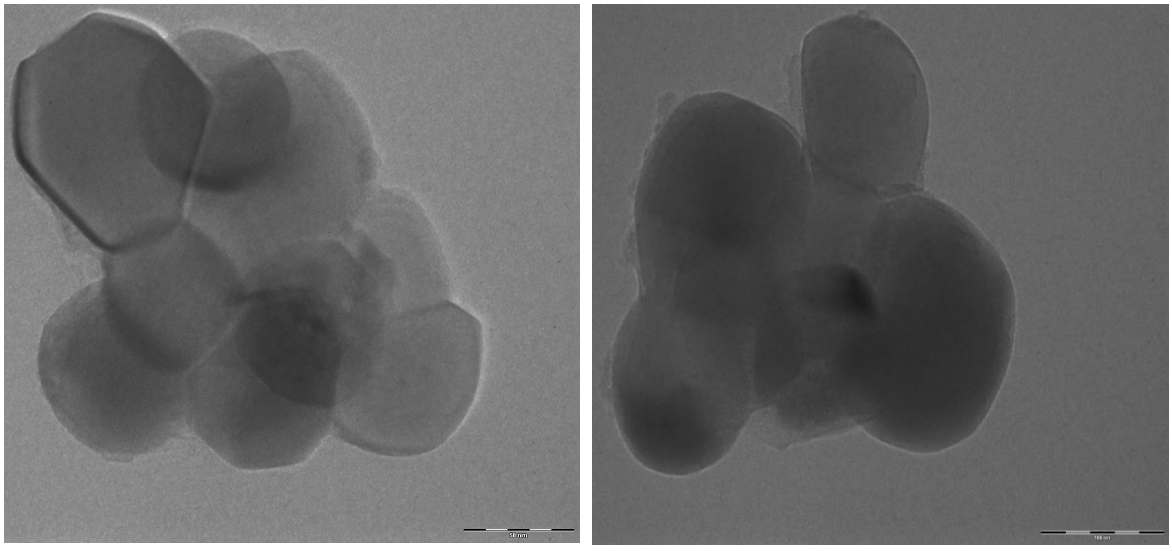

Figure 33. Transmission electron microscopy (TEM) image of H_3 and H_{33}.

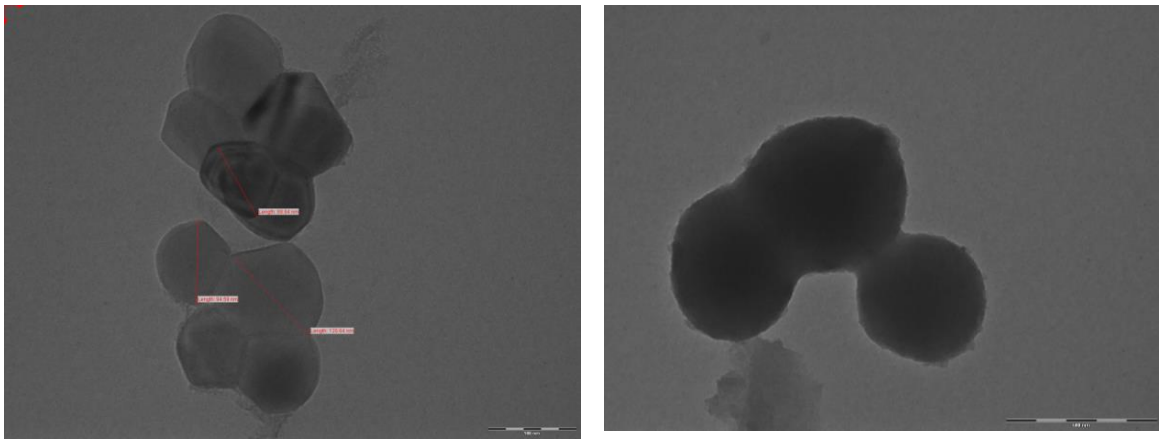

Figure 34. Transmission electron microscopy (TEM) image of H_4 and H_{44}.

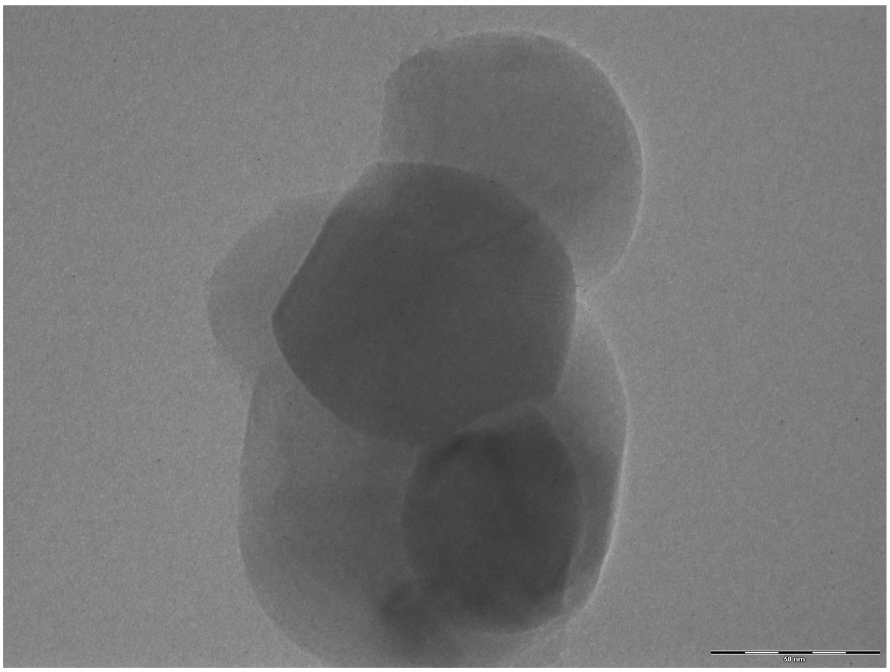

Figure 35. Transmission electron microscopy (TEM) image of H_{44}

From the above it is concluded that the particles are of almost uniformly of spherical and their size ranges in the order around 100 nm. Thus, in all the cases nanohybrids have been produced. Though in some cases it appears that some agglomeration of the particles also has taken place.

BET Surface Area Analysis

BET surface area characterization of the hybrid materials was carried out by N_2physiosorption at liquid nitrogen temperature. The results are presented in Table 8. The pore size has been calculated using Equation (3) as given below:

$$D = \frac{6\times10^3}{SA\times Density} nm \quad (3)$$

The calcination process has positive effect on the surface properties of the hybrid materials with a decrease in the pore size and an increase in the surface area. The calcined matrices of each hybrid series have better surface area and smaller pore size as compared to those of as-synthesized hybrid materials (Table 8). The increase in surface area is all due to the agglomeration of the particles which leads to the better stability of hybrid network structure.

Table 8. Surface area and pore size comparison data.

Hybrid Material	Density ($g\ cm^{-3}$)	Surface Area (m^2g^{-1})	Pore Size (*n*m)
Silica	2.65	458	4.943
Titania	4.23	45	31.520
Zirconia	5.68	80	13.204
Gelatin–silica hybrid	H_1 H_{11}	394.86 427.76	6.331 5.844
Modified gelatin–silica hybrid	H_2 H_{22}	426.62 453.53	7.647 7.208
Gelatin–titania hybrid	H_3 H_{33}	303.08 327.18	4.680 4.335
Gelatin–zirconia hybrid	H_4 H_{44}	324.61 414.16	3.256 2.551

CONCLUSIONS

The gelatin-based hybrid materials were prepared using the sol-gel approach, which is a method that shows promise and efficiency. In this paper, the synthesis of a series of gelatin-based hybrid materials was carried out using gelatin as the bio-polymeric backbone, silica, titania, or zirconia; SDS as surfactant for oil/water emulsion, TEOS as silylation or cross-linker material to obtain different hybrid materials for different applications. Consequently, four distinct types of gelatin-based hybrid materials were created: modified gelatin-silica hybrid, gelatin-silica hybrid, titanium hybrid, and gelatin-zirconia hybrid materials. The results of the EDS/EDX and CHNS analyses verified the hybrids' development. FTIR spectroscopy was used to characterize hybrid materials. The presence of additional absorption peaks of the functional groups of the biopolymeric components and changes in the location and intensity of the characteristic peaks of backbones in various networks indicate the modification of the backbone polymer or network formation. Morphological, XRD, and thermal characterization of the synthesized hybrid materials were also performed and these properties were also affected by the nature of the different inorganic materials used at the synthetic stage. The surface and internal particle surface morphology of different hybrids was compared from the SEMs and TEMs taken at different magnification. BET analysis was used to evaluate the surface area and pore size of the hybrid materials. It has been discovered that the hybrids' surface shape is influenced by the type of inorganic component and the circumstances of the reaction. The XRD investigation clarified how the hybrids' altered crystallinity caused the backbone structure to expand up. However, the various hybrid materials' thermal gravimetric study reveals that they are thermally more stable than pure gelatin. A novel procedure to enhance the surface and other characteristics of the materials that are synthesized is the calcination process. In conclusion, the materials that were created are mesoporous, high surface area, nano-hybrid materials that make excellent frontrunners for a variety of uses.

REFERENCES

1. Smitha S, Shajesh P, Mukundana P, Nair TDR, Warrier KGK. Synthesis of biocompatible hydrophobic silica–gelatin nano-hybrid by sol–gel process. Colloids Surf B: Biointerfaces. 2007; 55: 38–43.
2. Chujo Y, Saegusa T. Organic polymer hybrids with silica gel formed by means of sol-gel method. Adv Polym Sci. 1992; 100: 11–29.
3. Sanchez C, Ribot F, Lebeau B. Molecular design of hybrid organic-inorganic nanocomposites synthesized via sol-gel chemistry. J Mater Chem. 1999; 9: 35–44.
4. Sanchez C, Soler-Illia GJAA, Ribot F, Lalot T, Mayer CR, Cabuil V. Designed hybrid organic-inorganic nanocomposites from functional nanobuilding blocks. Chem Mater. 2001; 13: 3061–3083.
5. Sanchez C, Julian B, Belleville P, Popall M. Applications of hybrid organic-inorganic nanocomposites. J Mater Chem. 2005; 15: 3559–3592.

6. Chernev GE, Borisova BV, Kabaivanova LV, Salvado IM. Silica hybrid biomaterials containing gelatin synthesized by sol-gel method. Cent Eur J Chem. 2010; 8 (4): 870–876.
7. Nicole L, Rozes L, Sanchez C. Integrative approaches to hybrid multifunctional materials: from multidisciplinary research to applied technologies. Adv Mater. 2010; 22: 3208–3214.
8. Zamboulis A, Moitra N, Moreau Joel JE, Cattoen X, Man MWC. Hybrid materials: versatile matrices for supporting homogeneous catalysts. J Mater Chem. 2010; 20: 9322–9338.
9. Sanchez C, Rozes L, Ribot F, Laberty-Robert C, Grosso D, Sassoye C, Boissiere C, Nicole L. "Chimie douce": a land of opportunities for the designed construction of functional inorganic and hybrid organic-inorganic nanomaterials. C R Chim. 2010; 13: 3–39.
10. Gianotti E, Diaz U, Coluccia S, Corma A. Hybrid organic–inorganic catalytic mesoporous materials with proton sponges as building blocks. Phys Chem Chem Phys. 2011; 13: 11702–11709.
11. Warren SC, Perkins MR., Adams AM, Kamperman M, Burns AA, Arora H, Herz E, Suteewong T, Sai H, Li Z, Werner J, Song J, Werner-Zwanziger U, Zwanziger JW, Grätzel M, DiSalvo Francis J, Wiesner U. A silica sol–gel design strategy for nanostructured metallic materials. Nat Mater. 2012; 11: 460–467.
12. Chen Q, Miyaji F, Kokubo T, Nakamura T. Apatite formation on PDMS-modified CaO-SiO_2-TiO_2 hybrids prepared by sol-gel process. Biomaterials. 1999; 20 (12): 1127–1132.
13. Ren L, Tsuru K, Hayakawa S, Osaka A. Synthesis and characterization of gelatin-siloxane hybrids derived through sol-gel procedure. J Sol-Gel Sci Technol. 2001; 21: 115–121.
14. Schubert U. Silica-based and transition metal-based inorganic-organic hybrid materials – a comparison. J Sol-Gel Sci Technol. 2003; 26: 47–55.
15. Diaz U, Garcia T, Velty A, Corma A. Hybrid organic–inorganic catalytic porous materials synthesized at neutral pH in absence of structural directing agents. J Mater Chem. 2009; 19: 5970–5979.
16. Retuert J, Martinez Y, Quijada R, Yazdani-Pedram M. Highly porous silica networks derived from gelatin/siloxane hybrids prepared starting from sodium metasilicate. J Non-Cryst Solids. 2004; 347 (1–3): 273–278.
17. Ferreira RAS, André PS, Carlos LD. Organic–inorganic hybrid materials towards passive and active architectures for the next generation of optical networks. Opt Mater. 2010; 32 (11): 1397–1409.
18. Lei B, Shin KH, Noh DY., Jo IH, Koh YH, Choib WY, Kimb HE. Nanofibrous gelatin–silica hybrid scaffolds mimicking the native extracellular matrix (ECM) using thermally induced phase separation. J Mater Chem. 2012; 22: 14133–14140.
19. Reetz MT, Zonta A, Simpelkamp J. Efficient immobilization of lipases by entrapment in hydrophobic sol–gel materials. Biotechnol Bioeng. 1996; 49 (5): 527–534.
20. Schuleit M, Luis PL. Enzyme immobilization in silica-hardened organogels. Biotechnol. Bioeng. 2001; 72 (2): 249–253.
21. Soares CMF, Santana MHA, Zanin GM, Castro HFD. Covalent coupling method for lipase immobilization on controlled pore silica in the presence of nonenzymatic proteins. Biotechnol Prog. 2003; 19 (3): 803–807.
22. Shchipunov YA, Karpenko TY, Bakunina IY, Burtseva YV, Zvyagintseva TN. A new precursor for the immobilization of enzymes inside sol–gel-derived hybrid silica nanocomposites containing polysaccharides. J Biochem Biophys Methods. 2004; 58: 25–38.
23. Macario A, Moliner M, Corma A, Giordano G. Increasing stability and productivity of lipase enzyme by encapsulation in a porous organic-inorganic system. Microporous Mesoporous Mater. 2009; 118: 334−340.
24. Dragomirescu M, Vintila T, Preda G. Immobilized microbial cellulases in organic-inorganic hybrid materials. Anim Sci Biotechnol. 2011; 44 (1): 380–382.
25. Ren L, Tsuru K, Hayakawa S, Osaka A. Novel approach to fabricate porous gelatin–siloxane hybrids for bone tissue engineering. Biomaterials. 2002; 23: 4765–4773.
26. Vallet-Regí M, Balas F, Arcos D. Mesoporous materials for drug delivery. Angew Chem Int Ed. 2007; 46: 7548–7558.

27. Mahony O, Tsigkou O, Ionescu C, Minelli C, Ling L, Hanly R, Smith ME, Stevens MM, Jones JR. Silica-gelatin hybrids with tailorable degradation and mechanical properties for tissue regeneration. Adv Funct Mater. 2010; 20: 3835–3845.
28. Yanes RE, Tamanoi F. Development of mesoporous silica nanomaterials as a vehicle for anticancer drug delivery. Ther Deliv. 2012; 3 (3): 389–404.
29. Xu JH, Gao FP, Li LL, Ma HL, Fan YS, Liu W, Guo SS, Zhao XZ, Wang H. Gelatin–mesoporous silica nanoparticles as matrix metalloproteinases-degradable drug delivery system in vivo. Microporous Mesoporous Mater. 2013; 182 (1): 165–172.
30. Hu Q, Li J, Qiao S, Hao Z, Tian H, Ma C, He C. Synthesis and hydrophobic adsorption properties of microporous/mesoporous hybrid materials. J Hazard. Mater. 2009; 164: 1205–1212.
31. Qiu J, Wang Z, Li H, Xu L, Peng J, Zhai M, Yang C, Li J, Wei G. Adsorption of Cr(VI) using silica-based adsorbent prepared by radiation-induced grafting. J Hazard Mater. 2009; 166: 270–276.
32. Venditti F, Cuomo F, Ceglie A, Ambrosone L, Lopez F. Effects of sulphate ions and slightly acidic pH conditions on Cr(VI) adsorptions onto silica-gelatin composite. J Hazard Mater. 2010; 173: 552–557.
33. Jin X, Yu C, Li Y, Qi Y, Yang L, Zhao G, Hu H. Preparation of novel nano-adsorbent based on organic–inorganic hybrid and their adsorption for heavy metals and organic pollutants presented in water environment. J Hazard Mater. 2011; 186: 1672–1680.
34. Jin X, Li Y, Yu C, Ma Y, Yang L, Hu H. Synthesis of novel inorganic–organic hybrid materials for simultaneous adsorption of metal ions and organic molecules in aqueous solution. J Hazard Mater. 2011; 198: 247–256.
35. Zheng Y, Shengyang T, Jinxiang Y, Guangtao L. Mesoporous silicas functionalized with a high density of carboxylate groups as efficient absorbents for the removal of basic dyestuffs. J Mater Chem. 2006; 16: 2347–2353.
36. Arenas LT, Gay DSF, Moro CC, Dias SLP, Azambuja DS, Costa TMH, Benvenutti EV, Gushikem Y. Brilliant yellow dye immobilized on silica and silica/titania based hybrid xerogels containing bridged positively charged 1,4-diazoniabicyclo [2.2.2] octane: preparation, characterization and electrochemical properties study. Microporous Mesoporous Mater. 2008; 112: 273–283.
37. Lee KE, Morad N, Teng TT, Poh BT. Effects of different conditions on the removal of dye from reactive dye wastewater using inorganic-organic composite polymer. Int J Environ Sci Dev. 2012; 3 (1): 1–4.
38. Wang L, Wu X-L, Xu W-H, Huang X-J, Liu J-H, Xu A-W. Stable organic−inorganic hybrid of polyaniline/α-zirconium phosphate for efficient removal of organic pollutants in water environment. ACS Appl Mater Interfaces. 2012; 4: 2686−2692.
39. Moriones P, Rios X, Echeverria JC, Garrido JJ, Pires J, Pinto M. Hybrid organic–inorganic phenyl stationary phases for the gas separation of organic binary mixtures. Colloids Surf A. 2011; 389 (1–3): 69−75.
40. Guo W, Luo GS, Wang YJ. A new emulsion method to synthesize well-defined mesoporous particles. J Colloid Interface Sci. 2004; 271: 400–406.
41. Thakur SS, Chauhan GS. Gelatin–silica-based hybrid materials as efficient candidates for removal of chromium(VI) from aqueous solutions. Ind Eng Chem Res. 2014; 53 (12): 4838–4849. doi: 10.1021/ie401997g.
42. Thakur SS, Kumar A, Chauhan GS. Cellulase immobilization onto zirconia-gelatin-based mesoporous hybrid matrix for efficient cellulose hydrolysis. Trends Carbohydr Res. 2018; 10 (1): 45–55.
43. Thakur SS, Chauhan GS. Titania–gelatin-based nanohybrids: a versatile material for removal of organic dyes (Congo red, malachite green, crystal violet and methylene blue) from aqueous solution. In: Gupta B, Ghosh A, Suzuki A, Rattan S, editors. Advances in Polymer Sciences and Technology. Materials Horizons: From Nature to Nanomaterials. Singapore: Springer; 2018. pp. 147–176.doi: 10.1007/978-981-13-2568-7_14.

44. Sabataityte J, Oja I, Lenzman F, Volobujeva O, Krunks A. Characterization of nanoporous TiO_2 films prepared by sol-gel method. C R Chim. 2006; 9 (5–6): 708–712.
45. Birshtein VY, Tulchinskii VM. A study of gelatin by IR spectroscopy. Chem Nat Compd. 1982; 18 (6): 697−700.
46. Castro Y, Aparicio M, Moreno R, Duran A. Silica-zirconia sol–gel coatings obtained by different synthesis routes J Sol-Gel Sci Technol. 2005; 35: 41–50.
47. Olejniczaka MLZ, Cholewa-Kowalskab K, Wojtachb K, Rokitab M, Mozgawab W. ^{29}Si MAS NMR and FTIR study of inorganic–organic hybrid gels. J Mol Struct. 2005; 744: 465–471.
48. Chauhan GS, Kumar S, Kumari A, Sharma R. Study on the synthesis, characterization, and sorption of some metal ions on gelatin and acrylamide-based hydrogels. J Appl Polym Sci. 2003; 90: 3856–3871.
49. Smitha S, Mukundan P, Pillai PK, Warrier KGK. Silica–gelatin bio-hybrid and transparent nano-coatings through sol-gel technique. Mater Chem Phys. 2007; 103 (2–3): 318–322.
50. Spindloe C, The Production of Multi-Element Opacity Targets for X-Ray Laser Experiments, Target Fabrication: Laser Science and Development, Central Laser Facility Annual Report 2006/2007. Oxford, UK: Central Laser Facility. pp. 256–257.

